

YOUNG CORE COLLAPSE SUPERNOVA REMNANTS AND THEIR SUPERNOVAE

Roger A. Chevalier

*Department of Astronomy, University of Virginia, P.O. Box 3818,
Charlottesville, VA 22903; rac5x@virginia.edu*

ABSTRACT

Massive star supernovae can be divided into four categories depending on the amount of mass loss from the progenitor star and the star's radius: red supergiant stars with most of the H envelope intact (SN IIP), stars with some H but most lost (IIL, IIb), stars with all H lost (Ib, Ic), and blue supergiant stars with a massive H envelope (SN 1987A-like). Various aspects of the immediate aftermath of the supernova are expected to develop in different ways depending on the supernova category: mixing in the supernova, fallback on the central compact object, expansion of any pulsar wind nebula, interaction with circumstellar matter, and photoionization by shock breakout radiation. The observed properties of young supernova remnants allow many of them to be placed in one of the supernova categories; the major categories are represented. Of the remnants with central pulsars, the pulsar properties do not appear to be related to the supernova category. Models for young pulsar wind nebulae expanding into supernova ejecta indicate initial pulsar periods of 10 – 100 ms and approximate equipartition between particle and magnetic energies.

Subject headings: stars: neutron — stars: mass loss — supernovae: general — supernova remnants

1. INTRODUCTION

The discovery of the pulsar in the Crab Nebula showed that neutron stars are born in core collapse supernovae and that the PWN (pulsar wind nebula) is capable of sweeping up the immediately surrounding supernova ejecta. There has recently been a substantial increase in the number of observed young supernova remnants containing pulsars. In some cases, a pulsar was strongly suspected to be present, but was only discovered because of the increased sensitivity to pulsars afforded by new observatories such as the *ASCA* and *Chandra* X-ray observatories. These discoveries include PSR J0205+64 in 3C58 (Murray et al. 2002), PSR J1846–03 in Kes 75 (Gotthelf et al. 2000), PSR J1811–19 in G11.2–0.3 (Torii et al. 1997), PSR J1124–59 in G292.0+1.8 (Camilo et al. 2002a), and PSR J1930+19 in G54.1+0.3 (Camilo et al. 2002b). In addition to the PWN, the interaction of the supernova with its surroundings has been observed in some cases, showing

a variety of types of interaction. These combined observations give the possibility of relating the supernova remnant to the observed supernova types. It might also be expected that the properties of both the central neutron star and the surrounding PWN would depend on the type of supernova responsible for their formation.

In addition to the pulsar discoveries, there is also a growing class of compact central objects in supernova remnants that are not normal pulsars. These are likely to be neutron stars, and include radio quiet objects like the source in Cas A (Pavlov et al. 2000) and the AXPs (anomalous X-ray pulsars) such as the 12 s X-ray pulsar in Kes 73 (Vasisht & Gotthelf 1997). In cases where these occur in a young remnant (age ~ 1000 yr), there is the opportunity to investigate the supernova type.

Extensive supernova observations have clarified the various kinds of core collapse supernovae. Type IIP supernovae have a plateau light curve implying a massive H envelope, Type IIL have a linear light curve, Type IIn have narrow emission lines, SN 1987A-like have H in their spectra but are relatively faint and are powered by radioactivity at maximum, and Type Ib/c are lacking H and are also powered by radioactivity. The Type IIb supernovae, which are SNe II (Type II supernovae) that have the spectroscopic appearance of a SN Ib/c at late times appear to be undergoing strong mass loss and have a low mass H envelope at the time of the explosion. This is also true for the SNe IIL, which probably have more H envelope mass than a SN IIb, but less than is in the progenitor core. Type IIn supernovae typically also have strong mass loss, but the presence of narrow line emission may just depend on the sensitivity to detect lines (e.g., narrow lines were observed from SN 1987A). We thus consider 4 basic categories of core collapse supernovae: SN IIP, SN 1987A-like, SN IIL/b, and SN Ib/c. The first two categories end their lives with massive H envelopes and the next two have increasing amounts of mass loss.

Current information on supernova rates (Cappellaro et al. 1993, 1997) does not strongly constrain the relative rates of these events, although Cappellaro et al. (1997) find that SN 1987A-like events are not large contributors to the rate of core collapse supernovae. The *observed* rate of SNe IIL is comparable to that of SNe IIP (Cappellaro et al. 1993), but this might not reflect the intrinsic rate. From the theoretical point of view, Heger et al. (2003) have summarized results on the end point of massive single stars. In this view, Type IIP supernovae come from stars of mass $\sim 9 - 25 M_{\odot}$, SN Ib/c from mass $\gtrsim 35 M_{\odot}$, and SN IIL/b from the intermediate range. The rate of core collapse supernovae is strongly dominated by Type IIP events; the ratio of IIP to IIL/b rates is ~ 10 and IIP to Ib/c ~ 5 . In addition, almost all of the SNe IIL/b and a substantial number of SNe Ib/c undergo core fallback to a black hole and do not leave a neutron star. These relative numbers are changed if binaries make an important contribution to Type IIL/b and Ib/c supernovae, which is a good possibility (Nomoto et al. 1995; Wellstein & Langer 1999).

There is some observational information on the masses of stars that give rise to the various supernova types. Images of the sites of SNe IIP have led to upper limits on the mass of the progenitor of $15 M_{\odot}$ in 2 cases and $12 M_{\odot}$ in another (Smartt et al. 2003). A likely detection of

the progenitor of the Type IIP SN 2003gd leads to a zero age main sequence progenitor mass of $\sim 8 - 9 M_{\odot}$ (Van Dyk, Li, & Filippenko 2003). In the case of the Type IIb SN 1993J, the likely progenitor had an initial mass of $13 - 22 M_{\odot}$ (Van Dyk et al. 2002). The data on SNe IIP are consistent with the mass range expected for single stars. The mass of the SN 1993J progenitor is lower than expected in the single star scenario, but the likely binary companion has recently been detected (Maund et al. 2004). If SNe IIL/b and Ib/c came from single stars, more massive progenitors than for SNe IIP would be expected. From the observed fact that a higher fraction of SNe Ib/c occur in Sc galaxies than do SNe II, Cappellaro, Barbon, & Turatto (2004) infer a higher typical initial mass for the SNe Ib/c than for the SNe II. However, there may be considerable overlap in the initial masses for these events.

In addition to variations in the progenitor mass, there are variations in the supernova energy. Although most core collapse supernovae are inferred to have an explosion energy $\sim 1 \times 10^{51}$ ergs, there has recently been found a class of SNe with energies of a few 10^{49} ergs (Pastorello et al. 2004), as well as some SNe Ib/c and SNe IIn with energies up to a few 10^{52} ergs (e.g., Nomoto et al. 2001). The rate of the low luminosity and low energy supernovae could be up to 4 – 5% of the SN II rate (Pastorello et al. 2004).

The supernova type is important for determining the central conditions in a supernova. The compact core at the center of a core-collapse supernova can be affected by its immediate surroundings. An aim of the present paper is to examine whether the central evolution in the different kinds of core collapse supernovae and the different aspects of circumstellar interaction can lead to observable properties in the supernova remnant stage. In § 2, the density distribution, composition distribution, central mass fallback, circumstellar medium, and ionization at shock breakout for the various supernova types are examined. These properties can be important for the central compact object and its surrounding supernova remnant. The pulsar wind nebula interaction with surrounding supernova ejecta is treated in § 3. The shock wave interaction with a red supergiant wind is in § 4. These models are applied to young supernova remnants with pulsar wind nebulae in § 5 and to remnants without pulsar nebulae in § 6. Where possible, the remnant properties are used to identify the object with a supernova type. The conclusions are in § 7.

2. CORE COLLAPSE SUPERNOVA PROPERTIES

2.1. Density Distribution

Both the inner PWN interaction and the outer circumstellar interaction depend on the density structure of the supernova when it is in the free expansion phase, with a velocity profile $v = r/t$. This expansion phase should be reached within tens of days of the explosion, and the structure is expected to depend on the supernova type.

SN 1987A provides a well-studied case of an explosion of a BSG (blue supergiant) and is the

prototype of the SN 1987A-like class. Models show that the central density gradient is small, so the density can be expressed as $\rho_c = At^{-3}$, with $A \approx 10^9 \text{ g cm}^{-3} \text{ s}^3$ (Woosley 1988; Shigeyama & Nomoto 1990). This result is suitable for a star with mass $\sim 18 M_\odot$ in which the envelope mass is greater than the core mass, although there has been some mass loss. Another density estimate can be obtained from the analysis of Matzner & McKee (1999). For a star with a radiative envelope, the explosion leads to a density distribution with $\rho \propto r^{-1.06}$ at small radii. The typical velocity of interest for a PWN is about 1000 km s^{-1} , so the central density can be expressed as

$$\rho t^3 = 4.3 \times 10^8 \left(\frac{v}{1000 \text{ km s}^{-1}} \right)^{-1.06} \left(\frac{M_{ej}}{10 M_\odot} \right)^{1.97} E_{51}^{-0.97} \text{ g cm}^{-3} \text{ s}^3, \quad (1)$$

where M_{ej} is the ejected mass and E_{51} is the explosion energy in units of 10^{51} ergs. For SN 1987A, the result is similar to that given above. This expression is based on a harmonic mean analysis and misses some of the inner density structure (Fig. 10 of Matzner & McKee 1999), but this part of the supernova is likely to be affected by Rayleigh-Taylor instabilities in any case (Kifonidis et al. 2003 and references therein).

SNe IIP are expected to explode as RSGs (red supergiants) with their H envelopes nearly intact, giving rise to the extended plateau emission. Matzner & McKee (1999) give results for the 1-dimensional explosion of a $15 M_\odot$ star with its H envelope. In the free expansion phase, there is a central region with approximately constant density:

$$\rho t^3 \approx 2.4 \times 10^9 \left(\frac{M_{ej}}{15 M_\odot} \right)^{5/2} E_{51}^{-3/2}, \quad (2)$$

where the scalings with ejected mass M_{ej} and explosion energy E apply to stars with a similar initial density profile.

SNe IIL/b end their lives as red supergiants, but with small mass H envelopes because of mass loss. In this case, the stellar core gas is not effectively decelerated by the envelope, so the the inner density structure should approximate that of an exploded radiative core. Model 3H11 of Iwamoto et al. (1997) for the Type IIb SN 1993J has $M_{ej} = 2.06 M_\odot$, of which $1.95 M_\odot$ is in the core, and $E = 10^{51}$ ergs, so that eq. (1) implies a density of $1.7 \times 10^{-5} \text{ g cm}^{-3}$ at $t = 10^4$ s. The model at this time shows a central density of $\sim 10^{-5} \text{ g cm}^{-3}$ (Fig. 2 of Iwamoto et al. 1997), in approximate agreement with eq. (1). The expression for the explosion of a star with a radiative envelope can also be applied to SNe Ib/c. At the low mass extreme, the result for a star like the Type Ic SN 1994I with $M_{ej} \approx 0.9 M_\odot$ (Iwamoto et al. 1994), the coefficient in eq. (1) is 3.8×10^6 . This shows the likely range in the central density of a supernova.

The density estimates given here apply to the inner, relatively flat part of the supernova density profile. At higher velocities, the density gradient steepens, eventually going to a steep power-law profile (Matzner & McKee 1999). The profile begins to steepen at a characteristic velocity

$$v_b \approx 2 \left(\frac{E}{M_{ej}} \right)^{1/2} = 4500 E_{51}^{1/2} \left(\frac{M_{ej}}{10 M_\odot} \right)^{-1/2} \text{ km s}^{-1}. \quad (3)$$

At lower velocities, the density distribution is likely to be relatively flat, but have some clumpiness as a result of Rayleigh-Taylor instabilities. A more specific result for the transition velocity comes from assuming 2 power law segments ($\rho \propto r^{-m}$ on the inside and $\rho \propto r^{-b}$ on the outside) with a sharp break between them. The transition velocity is then (Chevalier & Fransson 1992)

$$\begin{aligned} v_{tr} &= \left[\frac{2(5-m)(b-5)}{(3-m)(b-3)} \frac{E}{M_{ej}} \right]^{1/2} \\ &= 3160 \left[\frac{(5-m)(b-5)}{(3-m)(b-3)} \right]^{1/2} E_{51}^{1/2} \left(\frac{M_{ej}}{10 M_{\odot}} \right)^{-1/2} \text{ km s}^{-1}. \end{aligned} \quad (4)$$

Matzner & McKee (1999) find that the outer density profile can be approximated by a steep power law, with $b = 10.2$ for a radiative star and $n = 11.7$ for a red supergiant. For a star with $m = 1.06$ and $b = 10.2$, the reference velocity becomes 3830 km s^{-1} .

An additional effect on the inner density distribution is that radioactive ^{56}Ni is present. Deposition of the radioactive power over a period of days and weeks results in the Ni bubble effect in which the radioactive material expands and sweeps up nonradioactive gas. The mass of ^{56}Ni present in an explosion, M_{Ni} , can be estimated from the late light curve. The case of SN 1987A is especially well-determined, with $M_{Ni} = 0.075 M_{\odot}$. Hamuy (2003) has estimated M_{Ni} in the range $0.002 - 0.26 M_{\odot}$ for 20 Type IIP supernovae; he found that the objects with higher M_{Ni} had higher explosion energies. Results for 7 Type Ib and Ic supernovae indicate $M_{Ni} = 0.07 - 0.15 M_{\odot}$ except for the highly energetic SN 1998bw with $M_{Ni} \approx 0.5 M_{\odot}$ (summarized by Hamuy 2003). We take $M_{Ni} = 0.1 M_{\odot}$ as a reference value and assume that ^{56}Ni is centrally located in region with a constant density distribution. Before the Ni bubble effect, the outer velocity of the region is thus

$$V_0 = 363 \left(\frac{M_{Ni}}{0.1 M_{\odot}} \right)^{1/3} \left(\frac{\rho_a t^3}{10^9 \text{ g s}^3 \text{ cm}^{-3}} \right)^{-1/3} \text{ km s}^{-1}. \quad (5)$$

The input of radioactive energy is $Q = 3.69 \times 10^{16} \text{ ergs g}^{-1}$ for $^{56}\text{Ni} \rightarrow ^{56}\text{Co}$ with decay time $\tau_d = 8.8$ days and an additional $7.87 \times 10^{16} \text{ ergs g}^{-1}$ for $^{56}\text{Co} \rightarrow ^{56}\text{Fe}$ with decay time $\tau_d = 110$ days. Radiative diffusion is likely to be important for most of the ^{56}Co decays, so we assume that the energy input can be approximated by that from ^{56}Ni decays. The outcome of the energy input is that the density of the Ni declines and sweeps up a shell with final velocity V_1 . Conservation of energy shows that (Basko 1994)

$$\left(\frac{V_1}{V_0} \right)^5 - \left(\frac{V_1}{V_0} \right)^2 = \frac{5Q}{V_0^2}. \quad (6)$$

A substantial Ni bubble effect requires that $5Q/V_0 \gg 1$ or

$$140 \left(\frac{M_{Ni}}{0.1 M_{\odot}} \right)^{-2/3} \left(\frac{\rho_a t^3}{10^9 \text{ g s}^3 \text{ cm}^{-3}} \right)^{2/3} \gg 1. \quad (7)$$

It appears that the effect is generally significant, except for a low mass Type Ic supernova. The

final velocity of the bubble region is

$$V_1 = 975 \left(\frac{M_{Ni}}{0.1 M_\odot} \right)^{1/5} \left(\frac{\rho_a t^3}{10^9 \text{ g s}^3 \text{ cm}^{-3}} \right)^{-1/5} \text{ km s}^{-1}, \quad (8)$$

and the density contrast between the matter inside the bubble with density ρ_b and the ambient gas is

$$\frac{\rho_b t^3}{\rho_a t^3} = 0.052 \left(\frac{M_{Ni}}{0.1 M_\odot} \right)^{2/5} \left(\frac{\rho_a t^3}{10^9 \text{ g s}^3 \text{ cm}^{-3}} \right)^{-2/5}. \quad (9)$$

The result can be an order of magnitude reduction of the central density. The assumptions that the Ni is centrally located and sweeps all the material into a shell lead to an underestimate of the actual Ni bubble effect. The shell is subject To Rayleigh-Taylor instabilities, but they probably have a small effect on the shell expansion (Basko 1994). More important is the fact that in a supernova like SN 1987A, the Ni is mixed out from the center during the explosion, so the result is a larger bubble with clumps of nonradioactive material inside the bubble.

2.2. Composition Distribution

The composition distribution of SN 1987A has been extensively investigated both theoretically and observationally. A crucial aspect of mixing is the Rayleigh-Taylor instabilities that occur when a denser core layer is decelerated by a lower density outer layer (Kifonidis et al. 2003 and references therein). The work of Kifonidis et al. (2003) included the density perturbations expected in a supernova driven by the neutrino mechanism, and they found that the instability in the Si/O interface is stronger than previous estimates. However, the instability at the He/H interface is weak because of the lack of significant perturbations in this region other than acoustic noise; the result is that little H is mixed into the core region. The observed late time line profiles of H α in SN 1987A show a centrally peaked line, implying that H is present at low velocity and that mixing to the center has occurred. In modeling the emission, Kozma & Fransson (1998) find that H has been mixed down to velocities $\lesssim 700 \text{ km s}^{-1}$. The inward mixing of H in SN 1987A is a puzzle as well as the outward mixing of Fe.

In models appropriate for SNe IIP, as in SN 1987A, the massive H envelope is able to decelerate the core material and the reverse shock wave carries H back toward the center. Shigeyama et al. (1996) note that that the He/C+O boundary is also unstable, but that the instability at the He/H boundary is much stronger and can mix in H to a velocity $\sim 1,000 \text{ km s}^{-1}$. However, the reverse shock front is delayed in arriving at the Si/Ni layer and there is little outward mixing of radioactive ^{56}Ni . These simulations include a 5% perturbation in the velocity field. Late spectral observations of the Type IIP SN 1999em show a very centrally peaked H α line, although the peak is redshifted by 400 km s^{-1} compared to the systemic velocity (Elmhamdi et al. 2003). There is again strong observational evidence for H mixing to close to the center.

The best studied case of a SN IIL/b is the Type Iib SN 1993J. Because of the low H envelope

mass, there is little deceleration of the core material and numerical simulations show relatively little mixing of the H into the core region (Iwamoto et al. 1997). The observed line profiles support this expectation; Houck & Fransson (1996) find that most of the H lies in the velocity range $8500 - 10,000 \text{ km s}^{-1}$. The O extends over the velocity $1000 - 4000 \text{ km s}^{-1}$, while the Fe extends out to 3000 km s^{-1} (Houck & Fransson 1996), showing that mixing between the inner core and the O region has occurred. SNe Ib/c have similarities to the SNe IIL/b in that there is little or no H envelope so that H from the envelope is not mixed to the center. There is likely to be mixing of the heavy element core material. From the [O I] line profile in the Type Ib SN 1985F, Fransson & Chevalier (1989) found that the distribution of O is broader than would be expected in a 1-dimensional model. However, there may be lack of O inside of 1000 km s^{-1} . It should be kept in mind that the supernova types are not distinct, but there is a continuous transition between the types.

Young PWNe have outer velocities $\sim 2000 \text{ km s}^{-1}$. At this level, the expected composition for SN IIP and SN 1987A-like events is a mixture of H envelope and core material. In the other supernova types, the H envelope material is absent and a mixture of core material is present. Lower velocity material ($\lesssim 500 \text{ km s}^{-1}$), relevant to the surroundings of central neutron stars, depends on the mixing back of outer material. The amount of mixing to these low velocities is uncertain in that the reverse shock wave may lose power because of outer shock breakout before the center is reached. In SN 1987A and the Type IIP SN 1999em, mixing of H very close to the center appears to have occurred.

2.3. Fallback

After an explosion is launched, some material can fall back to the central neutron star (Colgate 1971; Chevalier 1989). The nature of the fallback can depend on the supernova type.

Two types of fallback have been discussed. In the first, an outward explosion is generated in a star but the inner part of the flow falls back to the central object. Numerical simulations of this process show that it is sensitive to the energy and mass of the explosion (e.g., Herant & Woosley 1994; MacFadyen, Woosley, & Heger 2001). For a given energy, below a critical stellar mass, there is little effect, but above that mass, the effect becomes large (Herant & Woosley 1994).

A sudden change in the possible fallback is indicated by the blast wave self-similar solution for a $\gamma = 4/3$ flow in a medium with density profile $\rho = Dr^{-2}$ and a central mass M_c (Chevalier 1989). In this solution, there is a dimensionless constant, $\alpha = GM_c D/E$, where E is the energy. There is a critical value of $\alpha_c = 0.017$ below which the gas density goes to zero at the center and above which the density $\rightarrow \infty$. Allowing for a flow toward the neutron star because of neutrino losses, it is clear that the solutions with a high central density will have a much higher rate of fallback than the solutions with a low central density. Chevalier (1989) found that a $\rho = Dr^{-2}$ profile could approximate the central density in SN 1987A and that the corresponding value of α was less than,

but close to, α_c . The sharp change in behavior is consistent with the numerical results. If fallback occurs in this early phase, the material falling back is expected to be that just outside the compact core. If the object is in the strong fallback regime, the fallback is likely to cause collapse to a black hole. In the weak fallback regime, the amount of fallback is difficult to determine, as it depends on the explosion mechanism. Its composition is expected to be ^{56}Ni , along with ^4He .

The other mode of fallback involves matter that is brought back to the center by the reverse shock wave (see § 2.2). Based on a model for the central density in SN 1987A, Chevalier (1989) estimated a fallback mass in the reverse shock phase of $\sim 0.1 M_\odot$. However, the recent simulations by Kifonidis et al. (2003) show a considerably lower density right at the center; the simulations allow for accretion to a central compact object and the low accretion rates imply an accreted mass $\lesssim 0.001 M_\odot$ during the reverse shock phase. These results show there is a large uncertainty in the fallback mass. Any kick velocity of the neutron star could also affect its surroundings.

Chevalier (1989) suggested that the accreted mass from a normal SN IIP would be lower than in the case of SN 1987A because the more extended envelope would lead to accretion at a later time when the central density is lower. However, an examination of the central conditions at the time of the interaction at the O/He interface (e.g., Shigeyama & Nomoto 1990) indicates that the accreted mass at that time can be comparable to that occurring at the time of the He/H interaction. In this case, there may not be significant differences in fallback mass between the various core collapse supernovae except for the Type Ic supernovae that have lost much of their He region and have low mass accretion.

The angular momentum of the accreted material is important for the possible formation of a disk around the central object and for spinning up the neutron star. If the fallback material is from immediately around the neutron star, the angular momentum per unit mass is likely to be similar to that of the material going into the neutron star. However, if material is mixed down to the central region in connection with the reverse shock and Rayleigh-Taylor instabilities, the outer material is likely to have a higher angular momentum per unit mass, which can lead to disk formation. Even if a disk forms, there may be substantial pressure support in a disk that does not radiate efficiently, so we consider the accreted material to have a rotational velocity of βv_K , where v_K is the Keplerian velocity. If the neutron star rotates rigidly and is significantly spun up, the rotation period after the fallback accretion is

$$P_f \approx 4.6 \left(\frac{\Delta M}{0.1 M_\odot} \right)^{-1} \left(\frac{\beta}{0.5} \right)^{-1} I_{45} \text{ ms} \quad (10)$$

for a neutron star with $M = 1.4 M_\odot$ and $R = 10$ km, where I_{45} is the neutron star moment of inertia in units of 10^{45} g cm^2 . At the highest fallback mass estimates, the rotation of the neutron star can be substantial.

The fallback of material is also responsible for the composition on the surface of the remnant neutron star. In the cases of SN IIL/b and SN Ib/c, H from the envelope is not expected to be present, although material mixed down from the He zone might be present. In the case of SN IIP

and SN 1987A-like, H from the envelope might be accreted, depending on the efficiency of mixing downward by the Rayleigh-Taylor instability and the velocity of the neutron star.

2.4. Circumstellar Medium

Observations of supernovae at radio and X-ray wavelengths have given us a fairly complete picture of the immediate surroundings of core collapse supernovae (Chevalier 2003). This information can be useful for the identification of supernova types for young remnants because the initial interaction is with this material.

SN 1987A has a complex and well-studied circumstellar medium resulting from the late evolution to a RSG (red supergiant) and the subsequent evolution back to a blue supergiant (McCray 2003). The current interaction with the dense ring should continue for decades, after which the supernova shock wave will be propagating in the slow, dense wind from the red phase of evolution. The outer radius of the RSG wind is probably limited by the pressure, p , of the surrounding medium, and can be expressed as (Chevalier & Emmering 1989)

$$r_{RSG} = 5.0 \left(\frac{\dot{M}}{5 \times 10^{-5} M_{\odot} \text{ yr}^{-1}} \right)^{1/2} \left(\frac{v_w}{15 \text{ km s}^{-1}} \right)^{1/2} \left(\frac{p/k}{10^4 \text{ cm}^{-3} \text{ K}} \right)^{-1/2} \text{ pc}, \quad (11)$$

where k is Boltzmann’s constant. This outer boundary may have been observed as a shell around SN 1987A.

SNe IIP end their lives as red supergiants with relatively low mass loss rates. Pooley et al. (2002) deduced a mass loss rate $\sim (1 - 2) \times 10^{-6} M_{\odot} \text{ yr}^{-1}$ for $v_w = 10 \text{ km s}^{-1}$ for the Type IIP SN 1999em from X-ray and radio observations. This rate of mass loss is consistent with expectations for single stars of mass $\sim 10 - 15 M_{\odot}$ in the final phases of evolution (e.g., Schaller et al. 1992). Because of the low mass loss rate, the RSG wind extends to a relatively small distance from the progenitor, $\lesssim 1 \text{ pc}$ (eq. [11]). Outside of the RSG wind is a low density wind bubble created during the main sequence phase.

SNe IIL/b supernovae also end their lives as red supergiants, but with higher mass loss rates ($\gtrsim 3 \times 10^{-5} M_{\odot} \text{ yr}^{-1}$ for $v_w = 15 \text{ km s}^{-1}$) than the SNe IIP. The result can be a more extended dense circumstellar region, extending to 5 pc or more from the star. An interesting aspect of these supernovae is that the circumstellar medium frequently shows evidence for CNO processing, with an enhanced abundance of N. Fransson et al. (2004) summarize the evidence for SN 1979C (IIL), SN 1987A, SN 1993J (IIB), SN 1995N (IIn), and SN 1998S (IIL/n). The mass loss has been sufficiently strong to reveal layers where CNO processing has occurred.

SNe Ib/c are expected to have Wolf-Rayet star progenitors, which have typical values of $\dot{M} \sim 10^{-5} M_{\odot} \text{ yr}^{-1}$ and $v_w \sim 10^3 \text{ km s}^{-1}$ in our Galaxy. If the star had an earlier phase of RSG evolution, the dense wind from the RSG phase is expected to be swept up by the fast wind. For typical parameters, the mass loss rates for the the RSG and Wolf-Rayet phases are comparable, but

the Wolf-Rayet wind is 100 times faster than the RSG wind. The velocity of the swept up shell of RSG wind is expected to be 10 – 20 times the RSG wind velocity (Chevalier & Imamura 1983), or 100 – 200 km s⁻¹. The duration of the Wolf-Rayet phase spans a range, but a duration $\sim 2 \times 10^5$ yr is typical. The expectation is that the RSG wind is completely swept up by the Wolf-Rayet wind; after the interaction shock breaks out into the low density surrounding bubble, the swept up shell is subject to Rayleigh-Taylor instabilities, as found in numerical simulations (Garcia-Segura, Langer, & MacLow 1996). At the time of the supernova, the RSG wind material is in clumps at a radial distance $\gtrsim 10$ pc. An overabundance of N is a possible signature of the circumstellar origin of this material.

2.5. Ionization at shock breakout

Another aspect of the explosion that can depend on the supernova category is the amount of ionizing radiation that is emitted at the time of shock breakout. The emitting surface area is the most important parameter for the amount of radiated energy, so the radiative effects of shock breakout are largest for supernovae with red supergiant progenitors (Klein & Chevalier 1978). For standard values of the opacity and a density parameter, the amount of radiated energy at breakout for a red supergiant explosion is (Matzner & McKee 1999)

$$E_{rad} = 1.7 \times 10^{48} E_{51}^{0.56} \left(\frac{M_{ej}}{10 M_{\odot}} \right)^{-0.44} \left(\frac{R_*}{3.5 \times 10^{13} \text{ cm}} \right)^{1.74} \text{ ergs}, \quad (12)$$

where R_* is the radius of the progenitor. The strong dependence on R_* is clear. This expression should be applicable to both SNe IIP and SNe IIL/b. Because of mass loss, SNe IIL/b may typically have lower values of M_{ej} than the SNe IIP, which tends to give them larger values of E_{rad} because of the higher velocity of the breakout shock wave.

If the initial radiation is degraded to ionizing photons with an energy of 13.6α eV (with $\alpha > 1$), the number of ionizing photons is $7.8 \times 10^{58}/\alpha$ (for the reference values), which are capable of ionizing a hydrogen mass of $65 M_{\odot}/\alpha$. This shows that the ionizing radiation at the time of breakout can plausibly ionize the mass loss from the progenitor star in the red supergiant phase. This is not the case when the mass loss is so dense that the radiation dominated shock wave can be maintained in the circumstellar medium. Then the breakout occurs at such an extended radius that the emission is at optical wavelengths and is non-ionizing (e.g., Blinnikov et al. 2003). However, this presumably applies to only a small fraction of the red supergiant progenitors.

For a SN 1987A-like event, the reduced radius yields a number of ionizing photons $(2 - 3) \times 10^{57}/\alpha$ (Lundqvist & Fransson 1996; Matzner & McKee 1999), which have the capability of ionizing $\sim 2/\alpha M_{\odot}$ of H. In this case, the radiation may not be able to ionize all of the dense circumstellar mass. The case of SN Ib/c progenitors is even more extreme because the progenitor radius is $\sim 1 R_{\odot}$ and the energy in ionizing radiation is $\sim 10^{44} - 10^{45}$ ergs. In this case, only a small fraction of a M_{\odot} can be ionized and this mass is likely to be overrun early in the evolution of the supernova

remnant.

3. PULSAR WIND NEBULA INTERACTION

A first approximation to the PWN in hydrodynamic studies is that it can be treated as a constant pressure volume of $\gamma = 4/3$ fluid (Ostriker & Gunn 1971; Reynolds & Chevalier 1984; Chevalier & Fransson 1992; van der Swaluw et al. 2001). In a toroidal magnetic field model (Kennel & Coroniti 1984) there can be pressure gradients in the outer parts because of magnetic tension effects. However, the stability of such a configuration is doubtful, and polarization studies of PWNe indicate that the magnetic field does not have a purely toroidal configuration. In any case, the pressure at the outer contact discontinuity of the nebula does not depend on the detailed properties of the nebula (e.g., Bucciantini et al. 2003).

The basic equations for the evolution of the shell radius R , velocity V , mass M_s , and interior pressure p_i can be written

$$\frac{dR}{dt} = V, \quad \frac{dM}{dt} = 4\pi R^2 \rho_{sn} \left(V - \frac{R}{t} \right) \quad (13)$$

$$M \frac{dV}{dt} = 4\pi R^2 \left[p_i - \rho_{sn} \left(V - \frac{R}{t} \right)^2 \right] \quad (14)$$

$$\frac{d(4\pi R^3 p_i)}{dt} = L - p_i 4\pi R^2 \frac{dR}{dt}, \quad (15)$$

where ρ is the density in the freely expanding supernova ejecta and L is the power input from the central pulsar. For the evolution of L , we make the standard assumption of evolution with constant braking index n :

$$\dot{E} = \dot{E}_0 \left(1 + \frac{t}{\tau} \right)^{-(n+1)/(n-1)}. \quad (16)$$

The vacuum dipole value of n is 3, but observed values for pulsars are found to be smaller: 2.51 ± 0.01 for the Crab pulsar (Lyne et al. 1988); 2.837 ± 0.001 for PSR 1509–58 in MSH 15-52 (Kaspi et al. 1994); 1.81 ± 0.07 for PSR 0540–69 (Zhang et al. 2001); 2.91 ± 0.05 for PSR J1119–6127 in G292.2–0.5 (Camilo et al. 2000); and 1.4 ± 0.2 for the Vela pulsar (Lyne et al. 1996). The fact that there is a range of values of n indicates that the assumption of evolution with constant n is probably incorrect. Any conclusions that depend on this assumption should be viewed with caution. We make the assumption here in order to investigate the effects of pulsar power evolution and allow for various values of n .

As discussed above, the inner supernova density profile can reasonably be described by a power law $\rho_{sn} = At^{-3}(r/t)^{-m}$. Provided the pulsar is not a rapid rotator, the evolution of the nebula takes place in this part of the supernova. In this case, the evolution of the pulsar bubble

is described by the dimensional parameters A , \dot{E}_0 , and τ , and the dimensionless parameters n and m . Characteristic quantities for the radius, velocity, shell mass, and pressure can be found:

$$R_2 = \left(\frac{\dot{E}_0 \tau^{6-m}}{A} \right)^{1/(5-m)}, \quad V_2 = \frac{R_0}{\tau} = \left(\frac{\dot{E}_0 \tau}{A} \right)^{1/(5-m)}, \quad (17)$$

$$M_2 = (A^2 \dot{E}_0^{3-m} \tau^{3-m})^{1/(5-m)}, \quad P_2 = \left(\frac{A^3 \dot{E}_0^{2-m}}{\tau^{13-2m}} \right)^{1/(5-m)}. \quad (18)$$

These quantities can be used to nondimensionalize the basic variables

$$x = \frac{t}{\tau}, \quad y = \frac{R}{R_2}, \quad w = \frac{V}{V_2}, \quad z = \frac{M}{M_2}, \quad u = \frac{p_i}{P_2}. \quad (19)$$

Substitution into eqs. (13-15) yields

$$\frac{dy}{dx} = w, \quad \frac{dz}{dx} = 4\pi y^{2-m} x^{m-3} \left(w - \frac{y}{x} \right) \quad (20)$$

$$z \frac{dw}{dx} = 4\pi y^2 \left[u - y^{-m} x^{m-3} \left(w - \frac{y}{x} \right)^2 \right], \quad (21)$$

$$y^3 \frac{du}{dx} = \frac{1}{4\pi(1+x)^{(n+1)/(n-1)}} - 4y^2 u w. \quad (22)$$

In the limit $x \ll 1$, the power input is constant and the evolution can be solved analytically

$$y = B^{1/(5-m)} x^{(6-m)/(5-m)}, \quad w = \left(\frac{6-m}{5-m} \right) (Bx)^{1/(5-m)}, \quad (23)$$

$$u = \frac{1}{4\pi} \left(\frac{5-m}{11-2m} \right) B^{-3/(5-m)} x^{-(13-2m)/(5-m)}, \quad z = \frac{4\pi}{3-m} (Bx)^{(3-m)/(5-m)}, \quad (24)$$

where

$$B = \frac{(5-m)^3(3-m)}{4\pi(11-2m)(9-2m)}. \quad (25)$$

With this approximation, the radius of the PWN is (Chevalier & Fransson 1992; eq. [2.6])

$$R_p = \left[\frac{(5-m)^3(3-m)}{(11-2m)(9-2m)} \frac{\dot{E}}{4\pi A} \right]^{1/(5-m)} t^{(6-m)/(5-m)}. \quad (26)$$

For the particular case given in eq. (1) with $m = 1.06$, we have

$$R_p = 0.59 \dot{E}_{38}^{0.254} E_{51}^{0.246} \left(\frac{M_{ej}}{10 M_\odot} \right)^{-0.50} t_3^{1.254} \text{ pc}, \quad (27)$$

where $t_3 = t/(1000 \text{ yr})$. Another quantity of interest is the mass swept up by the PWN, which can be written

$$M_{sw} = \frac{(5-m)^3}{(11-2m)(9-2m)} \dot{E} R_p^{-2} t^3. \quad (28)$$

The coefficient is only weakly dependent on m , and for $m = 1.06$ is 1.0. The internal energy in the bubble is

$$\frac{E_{int}}{\dot{E}t} = \frac{5 - m}{11 - 2m}, \quad (29)$$

which is 0.44 for $m = 1.06$.

During the $x < 1$ phase, the swept-up shell is accelerated and is subject to Rayleigh-Taylor instabilities (Chevalier 1977; Jun 1998), which implies that after being shocked, the coupling between the PWN and the ejecta is reduced. In the extreme limit that there is no further acceleration of the ejecta after it is shocked, the left-hand side of eq. (14) drops out; there is direct pressure balance between the interior pressure and the ram pressure of the shock front. The solution for y , w , and u is similar to that given in eqs. (23) and (24), except that now

$$B = \frac{(5 - m)^3}{4\pi(11 - 2m)}. \quad (30)$$

Compared to the case where the ejecta are completely swept up, R is increased by a factor of 1.25 for $m = 0$ and 1.37 for $m = 1$. This is for the extreme limit, and the actual factor by which the radius is increased is likely to be smaller.

Once $x > 1$ ($t > \tau$), the power input from the pulsar drops and the swept up material tends toward free expansion. For $x \gg 1$, we have V and $M_{sw} \rightarrow$ a constant value. Consideration of eq. (22) shows that for $f \equiv (n + 1)/(n - 1) \geq 2$, $p_i \propto t^{-4}$ and for $f < 2$, $p_i \propto t^{-(2+f)}$. Results of integrating eqs. (20-22) are shown in Fig. 1 for the case of a swept up shell. The kinetic, E_{kin} , and internal, E_{int} , energies are normalized to the initial rotation energy of the pulsar, E_{rot} . The final energy is larger than E_{rot} because of the addition of kinetic energy of the supernova gas. Also shown is the instantaneous value of $\dot{E}t$, which may be observed for some cases. As expected, $\dot{E}t$ initially dominates, but becomes small for $t > \tau$, especially for low values of n . Measurements of $\dot{E}t$ and E_{int} in a young PWN can give an indication of the evolutionary phase of the pulsar. We find that $E_{int}/\dot{E}t$ becomes large for $t/\tau > 1$ and $(n + 1)/(n - 1) \geq 2$, and goes to a constant > 1 for $(n + 1)/(n - 1) < 2$.

The kinetic energy is less useful because the swept up mass is generally difficult to observe and may not be swept into an outer shell because of instabilities. The evolution of E_{int} can be found for the case of an unstable shell. Eqs. (23) and (24) show that during the early phase, $E_{int} \propto R^3 p_i \propto y^3 u$ has no dependence on B , so that E_{int} does not depend on whether the stable or unstable case applies. Integration of the differential equations to solve for the case $t > \tau$ shows that E_{int} remains very close to the stable case, so that the results given in Fig. 1 still apply.

These calculations can be used as follows when a PWN is still in the inner part of the supernova density profile. A lower limit on E_{int} can be estimated from the synchrotron emission; this limit occurs when there is approximate equipartition between the particles and magnetic field. With an estimate for the age t , the value of $\dot{E}t$ can be compared to E_{int} . A value of $E_{int}/\dot{E}t \gtrsim 1$ implies that the pulsar has undergone substantial spindown. The value of t/τ can be estimated for a given

value of $E_{int}/\dot{E}t$ for models with specified values of m and n . The results are not sensitive to the value of m for a plausible range, but they are quite sensitive to n ; values of t/τ are smaller for smaller n over a plausible range (1.5–2.8). Once t/τ is specified, the age and τ in the model are

$$t = \frac{2}{(n-1)} \left(\frac{t/\tau}{1+t/\tau} \right) t_{ch}, \quad \tau = \frac{2}{(n-1)} \frac{t_{ch}}{(1+t/\tau)}, \quad (31)$$

where $t_{ch} = P/(2\dot{P})$ is the observed characteristic spindown age of the pulsar. The value of t obtained this way must be checked for consistency with the value assumed for $\dot{E}t$. Once t/τ is determined, the initial values of \dot{E} and P are

$$\dot{E}_0 = \dot{E} \left(1 + \frac{t}{\tau} \right)^{(n+1)/(n-1)}, \quad P_0 = P \left(1 + \frac{t}{\tau} \right)^{-1/(n-1)}. \quad (32)$$

For many observed PWNe, the only other piece of observational data may be the radius of the nebula, R . Using the value of y corresponding to the value of x , we have

$$A = \frac{\dot{E}_0 \tau^{6-m} y^{5-m}}{R^{5-m}}. \quad (33)$$

This value of the central density parameter can be compared to the value expected in a supernova. For the case described by eq. (1), with $m = 1.06$, we have $A = 1.3 \times 10^{17} (M_{ej}/10M_\odot)^{1.97} E_{51}^{-0.96}$, where the numerical factor is in cgs units. Comparison with the value derived from the nebular model provides a consistency check on the model.

These considerations only apply while the PWN is in the inner, flat part of the supernova density profile. The time to reach the transition velocity, assuming constant power input, can be found by combining eqs. (4) and (26) and setting $v_{tr} = R_p/t$:

$$t_{tr} = \frac{2(b-5)(11-2m)(9-2m)}{(3-m)(5-m)^2(b-m)} \frac{E}{\dot{E}_0}. \quad (34)$$

For $b = 9$ and $m = 1$, we have $t_{tr} = 1.97E/\dot{E}_0$. In the case where a shell is not swept up because of instabilities, the bubble expands more rapidly and $t_{tr} = 0.56E/\dot{E}_0$ for $b = 9$ and $m = 1$. In either case, the condition is approximately $\dot{E}_0 t_{tr} \approx E$, or the energy injected by the pulsar must approximately be that of the expanding supernova gas; the energy required to displace the supernova gas is approximately the kinetic energy in the ejecta. The condition that the bubble reach the bend in velocity is thus that the initial pulsar rotational energy be greater than the kinetic energy in the supernova, or $I\Omega_0^2/2 > E$, where I is the moment of inertia of the pulsar and Ω_0 is its initial spin rate. This condition can be written as

$$P_0 < 9I_{45}^{1/2} E_{51}^{-1/2} \text{ ms}, \quad (35)$$

where I_{45} is the moment of inertia in units of 10^{45} g cm^2 .

If a PWN were able to expand past the inflection point in the supernova density profile where the profile becomes steeper than $\rho \propto r^{-5}$, there is a substantial difference in the evolution depending

on whether the swept-up shell breaks up by Rayleigh-Taylor instabilities. If the shell remains intact, the evolution is determined by the acceleration of a shell of fixed mass, with the result $R \propto t^{1.5}$ (Ostriker & Gunn 1971). However, if the shell breaks up, the expansion is determined by pressure equilibrium, with $R \propto t^{(6-m)/(5-m)}$. It can be seen that as $m \rightarrow 5$ or higher, the bubble expands rapidly into the low density medium and is expected to move out to the place where the outer parts of the supernova are interacting with the surrounding medium. In view of the expected Rayleigh-Taylor instability of the accelerated shell, the blow out scenario appears to be the most plausible (see also Bandiera, Pacini, & Salvati 1983).

In this section, we have neglected other sources of energy loss from the pulsar and PWN, such as gravitational radiation and radiative losses. For the initial periods found in § 5, gravitational radiation is not important. Radiative cooling may be important for the PWN at early times, but it is uncertain because it depends on the energy distribution of injected particles and the evolution of the distribution. The losses do not directly affect the magnetic field, which could drive the bubble expansion; however, a highly magnetized bubble may be subject to instabilities and magnetic reconnection. We briefly discuss radiative losses in § 5.10. There may be other modes of neutron star spindown at early times; however, if the injected power does work on the inner edge of the supernova ejecta, as assumed here, the process will affect the appearance of the PWN.

4. CIRCUMSTELLAR INTERACTION FOR SN IIL/b

As discussed in § 2.4, the circumstellar environment of massive stars is shaped by their mass loss and can be complex. In general, specific hydrodynamic models are needed to follow the mass loss interactions in the presupernova stage and the subsequent supernova (e.g., Dwarkadas 2001). Detailed models for individual supernova remnants are problematical because of the many parameters. One case that is more amenable to analysis is the case of a SN IIL/b interacting with the extended dense wind from the progenitor star. For the density profile of the exploded star, ρ_{sn} , we take the radiative star explosion model of Matzner & McKee (1999), with the profile in the harmonic mean approximation; eq. (1) represents the inner part of this density profile. The external medium is taken to be a freely expanding wind, with $\rho_{cs} = \dot{M}/4\pi r^2 v_w \equiv Dr^{-2}$. We define $D_* = D/1.0 \times 10^{14} \text{ g cm}^{-1}$, where the reference value corresponds to $\dot{M} = 3 \times 10^{-5} M_\odot \text{ yr}^{-1}$ and $v_w = 15 \text{ km s}^{-1}$. The circumstellar mass swept up to R is $M_{sw} = 9.8D_*(R/5 \text{ pc}) M_\odot$.

In the thin shell approximation, the equations for the evolution of the shell radius R , velocity V , and mass M_s are (Chevalier 1982)

$$\frac{dR}{dt} = V, \quad \frac{dM}{dt} = 4\pi R^2 \left[\rho_{sn} \left(\frac{R}{t} - V \right) + \rho_{cs} V \right] \quad (36)$$

$$M \frac{dV}{dt} = 4\pi R^2 \left[\rho_{sn} \left(\frac{R}{t} - V \right)^2 - \rho_{cs} V^2 \right]. \quad (37)$$

The parameters of the problem are E , M , and D , so dimensionless variables can be introduced:

$$x = \frac{t}{t_1}, \quad y = \frac{R}{R_1}, \quad w = \frac{V}{V_1}, \quad z = \frac{M}{M_1}, \quad (38)$$

where

$$R_1 = \frac{M_{ej}}{D}, \quad V_1 = \left(\frac{E}{M_{ej}} \right)^{1/2}, \quad M_1 = M_{ej}, \quad t_1 = \frac{R_1}{V_1} = \frac{M_{ej}^{3/2}}{DE^{1/2}}. \quad (39)$$

Substitution into eqs. (36-37) yields

$$\frac{dy}{dx} = w, \quad \frac{dz}{dx} = 4\pi \left[\frac{\rho_{sn}}{DR_1^{-2}} \left(\frac{y}{x} - w \right) y^2 + w \right], \quad (40)$$

$$z \frac{dw}{dx} = 4\pi \left[\frac{\rho_{sn}}{DR_1^{-2}} \left(\frac{y}{x} - w \right)^2 y^2 - w^2 \right], \quad (41)$$

where

$$\frac{\rho_{sn}}{DR_1^{-2}} = 0.0432x^{-3} \left[\left(\frac{w}{2.30} \right)^{0.236} + \left(\frac{w}{2.30} \right)^{2.261} \right]^{-4.5}. \quad (42)$$

The initial part of the evolution is dominated by the outer steep power law part of the supernova density profile. This part of the evolution is self-similar, with $y_{ss} = R_{ss}/R_1 = 1.314(t/t_1)^{0.878}$. The self-similar solution provides the initial conditions for the integration of eqs. (40-41).

The results of integrating eqs. (40-41) are shown in Fig. 2, where the deceleration parameter for the shell, s , is defined by $s = Vt/R$, M_{sej} is the ejecta mass swept into the shell, and M_{scs} is the circumstellar mass swept into the shell. It can be seen that the solution gradually evolves away from the early self-similar solution to a case with $s = 0.5$. This value of s is expected for the thin shell approximation, which is equivalent to the assumption of radiative shocks and momentum conservation at late times.

The thin shell approximation breaks down in the energy conserving case as the shocked region becomes broader; this transition is expected once the reverse shock front propagates back into the flat part of the supernova density profile. For an energy-conserving blast wave in a wind, the forward shock wave expands

$$R = (3E/2\pi D)^{1/3} t^{2/3} = 5.4E_{51}^{1/3} D_*^{-1/3} t_3^{2/3} \text{ pc}, \quad (43)$$

where $t_3 = t/(1000 \text{ yr})$. In terms of the variables used in this section, we have $y = 0.7816x^{2/3}$.

Typical values for the parameters are $E_{51} = 1$, $D_* = 1$, and $M_{ej} = 5 M_\odot$, leading to $R_1 = 32.1 \text{ pc}$, $V_1 = 3160 \text{ km s}^{-1}$, and $t_1 = 9930 \text{ yr}$. With these parameters, Fig. 3 shows results for the thin shell model (solid line) and the blast wave model (dashed line) over a radius-time range of interest. The blast wave case does not explicitly depend on M_{ej} but requires that the remnant be in an evolved state because of a low value of M_{ej} compared to the mass lost in the wind.

5. COMPARISON WITH OBSERVED PULSAR WIND NEBULAE

A list of probable young PWNe and supernova remnants in which central pulsars have been identified is given in Table 1; the list includes all of the objects, estimated to have an apparent age < 5 kyr, in Table 2 of Camilo et al. (2002a), except for N157B. One addition is the recently discovered pulsar in G54.1+0.3 (Camilo et al. 2002b). These objects are plausibly interacting with ejecta; N157B has an asymmetric morphology that suggests the PWN has interacted with the reverse shock front and is not considered here. References to the Galactic pulsar and remnant properties can be found in Green (2004). A recent reference to 0540–69 in the Large Magellanic Cloud is Hwang et al. (2001). The fourth column gives the current spindown power of the pulsar, $\dot{E} = 4\pi^2 IP^{-3}\dot{P}$, where I , the neutron star moment of inertia, is given in terms of $I_{45} = I/10^{45}$ g cm². The fifth column gives the observed pulsar period, P , and the sixth column gives the characteristic pulsar age, $t_{ch} = P/2\dot{P}$. If the pulsar is born rotating much more rapidly than the current rate and the braking index is $n = 3$, then t_{ch} is the actual age. If the pulsar is born with a period close to its current period, it can be younger than t_{ch} . Alternatively, if the pulsar is born spinning rapidly and has a braking index $n < 3$, it can be older than t_{ch} . The next two columns give the radii of the pulsar wind nebula and of the surrounding supernova remnant, if present. In some cases, the nebulae are asymmetric so that the quoted radius is a mean value.

As discussed in § 3, the internal energy in the PWN, E_{int} , can provide information of the evolutionary state of the nebula. The minimum internal energy, E_{min} , can be found from the synchrotron emission. PWNe typically have a moderately flat radio spectrum, with electron energy index $p_1 < 2$ and a steeper X-ray spectrum with energy index $p_2 > 2$. At some intermediate energy E_b , there is a break in the spectrum, at which the particles radiate at frequency ν_b . Most of the particle energy in the nebula is in particles with energies near E_b . Following Pacholczyk (1970), the energy in particles with $E < E_b$ is

$$E_{p1} = \frac{2c_1^{1/2}}{c_2(2-p_1)} \nu_b^{1/2} B_{\perp}^{-3/2} L_{\nu b}, \quad (44)$$

where $c_1 = 6.27 \times 10^{18}$ and $c_2 = 2.37 \times 10^{-3}$ (cgs units) are constants used in Pacholczyk (1970), B_{\perp} is the perpendicular magnetic field, and $L_{\nu b}$ is the spectral luminosity at ν_b . For a spectrum that is continuous across the break and that extends to high and low frequencies, we have $E_{p2}/E_{p1} = (2-p_1)/(p_2-1)$, where E_{p2} is the energy in particles above the break, leading to the total particle energy, $E_p = E_{p1} + E_{p2}$. The minimum energy condition is $E_B = (3/4)E_p$, where E_B is the magnetic energy. The minimum total energy ($E_p + E_B$) is then

$$E_{min} = 1.0 \times 10^7 \left(\frac{1}{2-p_1} + \frac{1}{p_2-2} \right)^{4/7} \nu_b^{2/7} R^{9/7} L_{\nu b}^{4/7} \text{ ergs}, \quad (45)$$

where cgs units are used. Estimates of E_{min} for the PWNe are given in Table 2, where the input parameters are also give. A related, but more complicated, expression for E_{min} is given in Blanton & Helfand (1996); they found $E_{min} = 9.9 \times 10^{47}$ ergs for Kes 75, which is in good agreement with

the value deduced here. The results are sensitive to the distance, d , with $E_{min} \propto d^{17/7}$. Also, there may more than one break between radio and X-ray wavelengths, or a more gradual turnover, which would reduce the value of E_{min} . As more observations become available on the spectra of PWNe, the energy estimates can be improved.

5.1. Crab Nebula

The abundances in the Crab Nebula point to an initial progenitor star in the $8 - 10 M_{\odot}$ range because of the lack of an O-rich mantle (Nomoto et al. 1982). This is likely to be in the range of the Type IIP supernovae, as indicated by recent observations of supernova progenitors (§ 1). For this type of supernova, core material is decelerated during the explosion and Rayleigh-Taylor instabilities mix H envelope gas to low velocities, as is observed in the Crab Nebula. The expansion of the pulsar nebula in a medium like that described by eq. (1) gives results that are in reasonable agreement with the observed properties of the Crab Nebula (Chevalier 1977; Chevalier & Fransson 1992).

As discussed in § 2.4, SNe IIP may have relatively weak winds during the progenitor red supergiant phase. The current radius of the Crab Nebula, 2 pc, is larger than the expected extent of the RSG wind and the forward shock should be at a considerably larger radius. Since the extent of the RSG mass loss is likely to be $\lesssim 1$ pc, the forward shock is currently in the low density surrounding bubble. Because the dominant source of X-ray emission is likely to be from gas that passed through a reverse shock at an earlier time and is now undergoing adiabatic expansion, detailed simulations are needed to show whether the expected emission would fall below observational limits. The ultimate test of models for the Crab is the detection of freely-expanding supernova gas or an interaction region outside of the well-observed PWN. $H\alpha$ emission is expected from the freely expanding ejecta and current upper limits are getting into an interesting range (Fesen et al. 1997).

5.2. 3C 58

Of the historical supernovae prior to 1500 AD, SN 1054 and SN 1006 have the most secure identifications with supernova remnants; in addition to positional agreement, the expansion of the remnants is consistent with the implied ages (Stephenson & Green 2002). Stephenson & Green (2002) also consider the identification of SN 1181 with 3C 58 to be secure, based on the length of time of Chinese observations, the position of the supernova and the lack of other viable candidates for the remnant. However, in this case the radio (Bietenholz, Kassim, & Weiler 2001) and optical (Fesen, Kirshner, & Becker 1988) expansion suggest an age greater than 820 years, although the smaller age is not ruled out if rapid deceleration has occurred.

An alternative point of view is that the remnant should not be identified with SN 1181 and is actually considerably older. Chevalier (2004) gave arguments for this being the case, based

on the PWN. These arguments were based on models with constant power pulsar period because $t_{ch} = 5390$ yr for 3C 58, which is much larger than the age of SN 1181. One argument is that currently $\dot{E}t < E_{int}$, implying that the pulsar has significantly spun down, which is inconsistent with the small age. Another is that the rapid expansion of the PWN requires lower density surrounding ejecta that can plausibly be expected, and is inconsistent with the $\sim 0.1 M_{\odot}$ inferred to be swept up, from X-ray observations (Bocchino et al. 2001).

In view of the evidence for spindown, the models of § 3 can be used to search for a consistent model for 3C58. Models can be found with $E_{int}/\dot{E}t = 0.7$ and ages of 3000 yr ($n = 2.8$) to 4000 yr ($n = 2.0$), which have $A \approx 1 \times 10^{17}$ and thus correspond to reasonable supernova parameters. Other parameters deduced from the models are $\dot{E}_0 \approx 1.3 \times 10^{38}$ erg s $^{-1}$ and $P_0 \approx 40$ ms, The internal energy in these models is $E_{int} \approx 5 \times 10^{47}$ ergs. The minimum energy for the synchrotron emission from 3C 58 is $E_{min} \approx 10^{48}$ ergs (Table 2), but there is probably a factor 2 uncertainty in this result. The models are incompatible with any strong deviation from the equipartition assumption; a higher value of E_{int} would be incompatible with typical supernova models.

The main problem with an age of 3000 – 4000 yr for 3C 58 is where, then, is the remnant of SN 1181; there are no plausible candidates at the expected position. However, some remnants with ages $\sim 10^3$ yr may be difficult to detect. The emission we observe from the Crab Nebula is essentially all due to the power from the Crab pulsar. If the central compact object were a low power pulsar or an object like that in Cas A, the supernova remnant could remain undetected.

With an age of several 1000 yr, the optical filaments and knots can be ejecta that have been overrun by the PWN. The knots are then expected to overlap the PWN, as observed. The presence of relatively slow, H-rich ejecta (Fesen, Kirshner, & Becker 1988) then suggests a SN IIP progenitor, as in the case of the Crab. The lack of observed interaction around 3C 58 can also be attributed to the low mass loss for this case.

5.3. 0540–69

The PWN in this object has already been examined in the context of interaction with freely expanding supernova ejecta (Reynolds 1985; Chevalier & Fransson 1992). Although the free expansion age for the nebula around the pulsar is 690 ± 45 years for a distance of 50 kpc (Kirshner et al. 1989), acceleration of the nebula by the pulsar bubble yields a somewhat larger age, ~ 830 years. The age is considerably less than the characteristic age of the pulsar, 1660 yr, so the nebula should be in the early stage of evolution. This is borne out by the ratio $E_{min}/\dot{E}t = 0.13(t/800 \text{ yr})^{-1}$. The ratio $E_{int}/\dot{E}t = 0.44$ is attained if E_{int} is several times the minimum energy. A realistic model must allow for some evolution; a model like that described in § 3 with $E_{int}/\dot{E}t = 0.58$, $m = 1.06$, and $n = 2.0$ yields $t = 790$ yr, $\tau = 2530$ yr, $\dot{E}_0 = 3.4 \times 10^{38}$ erg s $^{-1}$, $P_0 = 38$ ms, and $A = 2.2 \times 10^{16}$.

The remnant shows a larger shell in radio and X-ray emission, with some optical emission. The radio shell has a diameter of 17.5 pc (Manchester, Staveley-Smith, & Kesteven 1993), leading to a

mean velocity of 10,300 km s⁻¹ and implying that only high velocity ejecta have been decelerated by the surrounding medium. Despite the high mean velocity, the temperature of the X-ray emission is ~ 4 keV and the abundances are normal for LMC material (Hwang et al. 2001). These properties are consistent with the shock wave moving into a dense circumstellar shell. The presence of optical emission is indicative of dense clumps within the shell. As noted in § 2.4, a shell with these properties can be formed around a Wolf-Rayet star, which ultimately explodes as a SN Ib/c. If the shell is composed of material from a previous RSG phase, an overabundance of N might be expected. Mathewson et al. (1980) note that there is an arc of emission to the SW of the pulsar with strong [NII] emission, although the relation of the emission region to the supernova remnant is not completely clear.

In a SN Ib/c scenario, slow moving ejecta around the PWN should be free of H. The presence of H α emission in the inner nebula has been controversial (Dopita & Tuohy 1984; Kirshner et al. 1989), but the absence of H β emission is consistent with the H-free hypothesis. The absence of H α emission in the inner nebula is a prediction of the scenario proposed here.

5.4. Kes 75

The pulsar in Kes 75 is notable for its short characteristic age, $P/2\dot{P} = 723$ years; however, the actual age is uncertain because of the uncertain amount of spindown and the uncertain braking index (Helfand, Collins, & Gotthelf 2003). There are signs that the pulsar has undergone substantial spindown. One is that currently $\dot{E}t = 2.5 \times 10^{47} t_3$ ergs, where t_3 is the age in 10^3 yr, whereas the minimum energy in fields and particles in the synchrotron nebula is 1×10^{48} ergs (Blanton & Helfand 1996; Table 2). We have $E_{int}/\dot{E}t \approx 4$ if the particles and fields are close to equipartition and higher if not. Figure 1 shows that this is an indication of an evolved pulsar. Another indication is the size of the PWN. The size of the synchrotron nebula in Kes 75 is comparable to that in 0540–69, although the current \dot{E} is smaller by a factor of 18.

The model described in § 3 has been used to search for a consistent model for Kes 75, assuming the inner supernova density profile given by eq. (1). For n in the range 2.0 – 2.8, we found a set of models with $E_{int}/\dot{E}t \approx 4$ that yield $A \approx 1 \times 10^{17}$ (within a factor of 2), which is consistent with expansion in a normal supernova. The value of P_0 in these models is ~ 30 ms. Other model results show more variation with $t = 1300, 940, 800$ yr, $\tau = 140, 27, 8.4$ yr, and $\dot{E}_0 = 8.6 \times 10^{39}, 3.3 \times 10^{40}, 1.3 \times 10^{41}$ erg s⁻¹, for $n = 2.0, 2.5, 2.8$, respectively.

Kes 75 has an outer shell structure at X-ray and radio wavelengths that is similar to that observed in 0540–69 (Helfand et al. 2003). The shell radius is 9.7 pc, so that the mean expansion velocity is $9,500t_3^{-1}$ km s⁻¹. As in the case of 0540, the large mean velocity is suggestive that the supernova has traversed a region of low density and is now interacting with a higher density shell. These properties are indicative of a SN Ib/c.

5.5. MSH 15-52

This remnant is notable for its large size relative to its age. Radio emission to the SE of the pulsar is at a distance of 25 pc from the pulsar (for a distance of 5.2 kpc, Gaensler et al. 1999). For an age of 1700 yr, the characteristic spindown time of the pulsar, the mean velocity to this region is $14,000 \text{ km s}^{-1}$, suggesting that the supernova ejecta have traveled relatively unimpeded to this region. Gaensler et al. (1999) argue for a high E/M ratio and a SN Ib/c origin. This supernova type is plausible and we build on that scenario here.

The PWN itself is large and of low surface brightness in X-rays, and is not clearly observed at radio wavelengths. With the current $\dot{E} = 1.8 \times 10^{37} I_{45} \text{ erg s}^{-1}$, we have $\dot{E}t = 9.7 \times 10^{47} I_{45}(t/1700 \text{ yr}) \text{ ergs}$, which can be compared to the minimum energy estimate of $1.5 \times 10^{48} \text{ ergs}$ (Table 2). This estimate is quite uncertain because of the uncertain radio observations and the possibility that the spectrum flattens just below X-ray wavelengths (Gaensler et al. 2002). The additional constraint of expansion into a plausible supernova surrounding medium shows that significant evolution (i.e. spindown) of the pulsar is needed. The point is that considerable energy is needed for the PWN boundary to have expanded to such a large size and fairly rapid initial rotation of the pulsar is indicated, unless the surrounding supernova has extremely low mass or high energy. As an example, a model with $n = 2.8$ and $E_{int}/\dot{E}t = 4$ yields $t = 1870 \text{ yr}$, $\tau = 19 \text{ yr}$, $E_0 = 3 \times 10^{41} \text{ erg s}^{-1}$, $P_0 = 12 \text{ ms}$, and $A = 3 \times 10^{16}$ in cgs units. The internal energy is 2 – 3 times the equipartition value. This model is comparable to that proposed in Chevalier & Fransson (1992).

The optical knots that comprise RCW 89, that are presumably emitting by supernova interaction, are at a distance $\gtrsim 10 \text{ pc}$ from the pulsar. In the SN Ib/c explosion scenario, they are possibly material in the RSG wind that was swept up during the Wolf-Rayet phase (§ 4). The strong [NII] lines from this gas (Seward et al. 1983) provide support for this identification.

The model for the PWN gives an age that is consistent with the remnant originating in SN 185. In particular, the evidence for strong spindown and the braking index near 3 imply an age within about 200 yr of $t_{ch} = 1700 \text{ yr}$.

5.6. G292.0+1.8

At a distance of 6 kpc (Gaensler & Wallace 2003), the $8'$ diameter of the remnant corresponds to a radius of 7 pc. The presence of O-rich, H-poor filaments at a velocity of $\sim 2000 \text{ km s}^{-1}$ (Murdin & Clark 1979) immediately places the supernova in the IIL/b or Ib/c categories. The interaction is presumably with the RSG wind of the progenitor star, and the current radius indicates that the shock front is in the outer parts of the wind, implying a Type IIL/b identification. The structure that is observed in the outer X-ray emission, such as the filament of emission across the E–W direction (Park et al. 2002) is probably structure in the RSG wind; this is consistent with the

normal abundances found in this region.

The displacement of the PWN from the center of the supernova remnant can be interpreted as implying a kick velocity of the neutron star of $\sim 480 \text{ km s}^{-1}$ for a distance of 6 kpc and an age of 3200 yr (Hughes et al 2001). Alternatively, the displacement may be the result of an asymmetric interaction with the circumstellar medium, as appears to be the case with Cas A (Reed et al. 1995). In either case, the pulsar is surrounded by uniformly expanding supernova ejecta, so that the models of § 3 apply, provided that there is not a strong radial density gradient in the ejecta. Taking a distance of 6 kpc and $R = 3.5 \text{ pc}$ for the PWN (Gaensler & Wallace 2003), we have calculated a number of models with $n = 2.0, 2.5, 2.8$. In order to obtain $A \approx 10^{17}$, the models have ages of 2700 – 3700 yr, $P_0 = 30 - 45 \text{ ms}$, and $\dot{E}_0 = (3 - 30) \times 10^{38} \text{ erg s}^{-1}$.

The internal energy in the models is $(1 - 2) \times 10^{48}$ ergs, which can be compared to the minimum energy of $E_{min} = 1 \times 10^{48}$ ergs (Table 2). Hughes et al. (2003) estimate an internal energy $\sim 4 \times 10^{49}$ ergs, based on the assumption that the similar extent of radio and X-ray emission implies that the synchrotron lifetime of the particles is comparable to the age. The results of § 3 show that the kinetic energy of the nebula would have to be much larger than E_{int} when $E_{int}/\dot{E}t > 30$. For $n = 2$, the value of E_{kin} would be $\sim 4 \times 10^{51}$ ergs and would be larger for larger values of n . Not only is this energy surprisingly large, but the size of the PWN would be larger than observed for any plausible age and supernova density. These considerations suggest that the value of E_{int} is closer to the equipartition value and that the X-ray extent is not an indicator of particle lifetimes.

The strong interaction that the remnant shows out to the outer shock wave at $R = 7 \text{ pc}$ can be interpreted in terms of interaction with the dense wind expected to be present around a Type III/b supernova. The radius is close to the maximum extent that is expected for such a wind (§ 2.4). Ghavamian et al. (2002) have detected clumpy photoionized gas that is superposed on the remnant. The fact that it does not extend out beyond the remnant shows that the shock front is likely to be close to the edge of the RSG wind and may be interacting with a shell at the edge of the wind. The X-ray luminosity suggests a swept up mass of $\sim 7 - 8 M_\odot$ (Gonzalez & Safi-Harb 2003a), which is consistent with a RSG wind. For the reference wind parameters used before ($\dot{M} = 3 \times 10^{-5} M_\odot \text{ yr}^{-1}$ and $v_w = 15 \text{ km s}^{-1}$), the swept up mass is $13.7(R/7 \text{ pc}) M_\odot$. The wind interaction models of § 4 can be used to test the radius and age for consistency. Fig. 3 shows that the remnant’s properties are roughly consistent with those expected in the interaction models.

The fact that heavy element rich knots with velocities $\gtrsim 1000 \text{ km s}^{-1}$ have been observed (Murdin & Clark 1979) supports the Type III/b identification. However, the age of ~ 3200 yr deduced in the present model is greater than the $\lesssim 1600$ yr estimated by Murdin & Clark (1979) from the knot velocities. Murdin & Clark obtained their limit by dividing the observed velocity range (2030 km s^{-1}) into the 3.0 pc diameter that they estimated for the remnant. The emitting knots could actually be within the 14 pc diameter of the outer shock front (Gaensler & Wallace 2003), which gives an age limit of < 6700 yr. This limit can be reduced by considering the

asymmetry in the line profiles and projection effects; a study of the fast optical knots has the potential to yield a realistic age estimate for the remnant.

5.7. G11.2–0.3

This remnant is another excellent case of both a PWN and circumstellar shell interaction. At a distance of 5 kpc (Green et al. 1988), the radius of the remnant is 3.3 pc, so the RSG wind is an immediate candidate for the interaction, which places the remnant in the Type IIL/b category. Green et al. (1988) find that the radio emission does not have a well-defined outer edge, so the outer shock front could be at a larger radius. The PWN is not symmetric, but its radius can be approximated as 0.9 pc (Tam, Roberts, & Kaspi 2002). Clark & Stephenson (1977) suggested that G11.2–0.3 is the remnant of SN 386. Stephenson & Green (2002) note that the information on this event does not conclusively identify it as a supernova and that there are other candidate supernova remnants; however, it appears to be the remnant in the region with the smallest diameter and largest surface brightness. The identification with SN 386 and the remnant’s small size imply an age much less than the pulsar spindown age of 24,000 yr (Torii et al. 1999), which suggests that the current pulsar period and power are close to their initial values.

Taking the age to be 1618 yr, we have $\dot{E}t = 3.3 \times 10^{47} I_{45}$ ergs, to be compared to the minimum energy in particles and fields $E_{min} \approx 3 \times 10^{46}$ ergs (Table 2). With a steady input of energy, we expect $E_{int}/\dot{E}t = 0.45$ and, in this case, $E_{min}/\dot{E}t = 0.1$, so there is no problem in the pulsar producing the internal energy in the PWN. Some deviation from equipartition is indicated; the alternative is that the remnant is younger than SN 386. Substituting the age and \dot{E} into eq. (28) yields $R_{PWN} = 0.54 E_{51}^{0.246} (M_{ej}/10 M_{\odot})^{-0.5}$ pc. Compared to the observed value of 0.9 pc, a small value of the ejected mass is indicated, although uncertainties in the model (due to, e.g., the asymmetry of the nebula) do not make it possible to conclude more than that the observations are roughly consistent with model expectations.

Fig. 3 shows that the small size of G11.2–0.3 is consistent with an origin in SN 386 if it is compared to the thin shell model. In this case, the deceleration parameter is $m = 0.66$ for the standard parameters. This value applies to the whole shell because of the thin shell approximation, although the reverse shock is expected to have a lower value of m than the forward shock. From radio observations, Tam & Roberts (2003) deduced $m = 0.68 \pm 0.14$ (20 cm observations) and $m = 0.48 \pm 0.16$ (6 cm observations). The agreement with the model value is adequate.

5.8. G54.1+0.3

This object has the interesting feature that the pulsar has similar properties (P and \dot{P}) to the one in G292.0+1.8, but it is lacking the surrounding circumstellar interaction. There are also differences in the PWNe, with G54.1+0.3 being considerably less luminous at radio wavelengths

and having a smaller size. Considering that other PWNe appear to have E_{int} close to E_{min} , that $E_{min} = 8 \times 10^{46} d_5^{17/7}$ ergs (Table 2) where d_5 is the distance in units of 5 kpc, and that $\dot{E}t = 3.8 \times 10^{47} I_{45} t_3$ ergs, the indications are that G54.1+0.3 is in an early evolutionary phase, with an age $< \tau_{ch} = 2900$ yr. Substituting $\dot{E}_{38} = 0.12$ and $M_{ej} = 5 M_\odot$ in eq. (28) yields $R = 0.5 t_3^{1.254}$ pc for the swept up shell case and $R = 0.7 t_3^{1.254}$ pc for the unstable case. \dot{E}_{38} should be somewhat larger than 0.12 because of evolution, but this does not substantially change the results. The indications are that $t \approx 1500$ yr and $P_0 \approx 100$ ms, using the relations from § 3. This examination of the PWN shows that although this pulsar and the one in G292.0+1.8 have similar magnetic fields, the one in G54.1+0.3 was born with a significantly larger period and is younger. The differences between the PWNe cannot be attributed solely to different supernova surroundings because the ratio $E_{int}/\dot{E}t$ depends only on t/τ and n , and not on the supernova properties.

Given the age of G54.1+0.3 and the lack of strong circumstellar interaction, a Type IIL/b supernova is ruled out. Beyond that, there are at present no further clues on the supernova type. The similarity to the Crab and 3C58 is suggestive of Type IIP, but a Type Ib/c is also possible.

5.9. PSR J1119–6127 and G292.2–0.5

The pulsar PSR J1119–6127 and its surrounding remnant G292.2–0.5 are notable in that the emission from any PWN is very weak (Crawford et al. 2001; Gonzalez & Safi-Harb 2003b). Crawford et al. (2001) argue that the reason for the weak emission is that the initial spindown time, τ , was small because of the high magnetic field, so that the internal energy suffered strong adiabatic losses after the initial period of energy injection. We concur with this suggestion.

The radius of the G292.2–0.5 supernova remnant is $10.9 d_5$ pc, where d_5 is the distance in units of 5 kpc; the distance is poorly known and may be in the range 2.5 – 8 kpc (Crawford et al. 2001). The size of the remnant and the relatively small X-ray luminosity, $(3 - 4) \times 10^{35}$ erg s⁻¹ (Pivovarov et al. 2001), suggest that the remnant is not a Type IIL/b, again leaving the IIP and Ib/c categories.

5.10. Discussion

The basic results on supernova type and pulsar properties are given in Table 3. The suggested types are from the 3 main supernova categories and, in this picture, the main factor in determining the appearance of a young supernova remnant with a pulsar is the category of the initial supernova. For the supernova identifications, the circumstellar interaction plays an important role and can be most clearly seen in the Type IIL/b and Ib/c events. For the putative Type IIP events identified here, no circumstellar interaction has been definitely observed, so there remains some doubt on the identification. Another important indicator of supernova type is the composition of the ejecta, with the presence of slow H distinguishing the IIP from the IIL/b and Ib/c events. In some cases,

optical emission from the ejecta may be from just a small fraction of the mass, so it is necessary to assume that the observed emission is representative of gas at that velocity.

X-ray observations of the supernova remnant shells contain information on the explosion interactions, but element abundances, inhomogeneities, and time-dependent effects are important for the interpretation, which is beyond present considerations. The X-ray luminosities of the Type IIL/b events are $L_x \sim 1 \times 10^{37}$ erg s⁻¹, which is higher than the values for the SNe Ib/c (with $L_x \lesssim 3 \times 10^{36}$ erg s⁻¹), except for Kes 75 with $L_x \approx 1.8 \times 10^{37}$ erg s⁻¹ (Helfand et al. 2003). The Type Ib/c events have harder X-ray emission than the IIL/b events, as expected with their higher mean velocities.

Errors in the ages and values of P_0 are difficult to estimate because of the uncertain pulsar spin evolution and the detailed properties of the surrounding supernova. Running a variety of models for individual objects indicates an uncertainty of order 30%.

In general, the PWN models show that the observed nebulae are consistent with a nebula within a factor of a few of energy equipartition between particles and magnetic fields expanding into the inner, freely expanding ejecta of a supernova. There is not a clear theoretical reason for energy equipartition, although Rees & Gunn (1974) note that there may be a mechanism that keeps the magnetic field from becoming larger than the equipartition value.

The estimates of initial periods are in the range 10 – 100 ms, although there is some concentration around 40 ms. In cases where the current period is > 100 ms, there is evidence for an initial period that is significantly smaller. The range of initial periods is comparable to the values deduced by van der Swaluw & Wu (2001) for older remnants in which the reverse shock wave has compressed the pulsar wind nebula. One way out of this constraint would be if there were an early radiative phase of the PWN. For a radiative phase lasting $\lesssim 10^3$ yr, the luminosity would be $\gtrsim 6 \times 10^{39}$ erg s⁻¹ in order for the initial period to be < 10 ms. This luminosity should be accessible in supernova observations, but steady luminosities of this order have not been reported, so that rapid initial rotation cannot be accommodated in this way.

Table 3 also gives estimates of the current magnetic fields of the pulsars, based on observations of P and \dot{P} . It can be seen that neither the magnetic field nor the initial periods of the pulsars show a clear trend with supernova type. There are possible reasons for a dependence of the stellar rotation on the supernova category. Mass loss from a star is expected to carry away angular momentum, which could result in slow central rotation. On the other hand, binary interaction, which might be important for the IIL/b and Ib/c categories, can increase the angular momentum of a star. The results found here do not show evidence for one of these effects being dominant.

Provided it is not changed by surface nuclear processing, the atmospheric composition of a young neutron star should reflect the composition of the fallback material, which can vary in the different supernova types. H is expected in SNe IIP, but not in the types with considerable mass loss. Slane et al. (2004) find that X-ray observations of the neutron star in 3C 58 are consistent with a light element atmosphere, as can occur in a SN IIP by fallback.

6. SUPERNOVA REMNANTS WITH NON-PULSAR COMPACT OBJECTS

An important development in recent years has been the discovery of compact objects that are not normal radio or X-ray pulsars. These objects have not been detected as radio sources and in cases where X-ray pulsations are seen (Anomalous X-Ray Pulsars), the period is relatively long (~ 12 s). Although the central objects do not generate observable nebulae, a number of them are surrounded by young supernova remnants, which can be analyzed for their supernova type. The young remnants (ages $\sim 10^3$ yr) are listed in Table 4.

6.1. Cassiopeia A

The compact object in Cas A belongs to the class of central objects with thermal X-ray emission, no observable pulsations, and no surrounding nebula (Pavlov et al. 2000). The case for Cas A being a SN IIL/b was made in Chevalier & Oishi (2003). The positions and expansion rates of the forward and reverse shock waves can be explained by interaction with a wind. Outside of the outer shock front is material that can be identified with clumpy wind gas that was photoionized by the burst of radiation from the time shock breakout; it extends to a radius of 7 pc.

6.2. RCW 103

This remnant was one of the first showing a non-pulsar central compact object. The X-ray source shows strong variability, but no pulsations (Gotthelf et al. 1999). The distance to the remnant from recent HI absorption line studies is found to be between 3.1 and 4.6 kpc (Reynoso et al. 2004); we take a distance of 3.8 kpc. The radius of the X-ray SNR is $3'.5$, or 5.0 pc.

The remnant radius is in a range where it may still be interacting with mass loss from the RSG phase. Support for this hypothesis comes from an apparent overabundance of N observed in cooling shock waves at the outer edge of the remnant (Ruiz 1983). However, the density of a free wind at 5.0 pc would be $\rho = 4 \times 10^{-25}$ g cm $^{-3}$ for $D_* = 1$, which is too low to produce the radiative shock waves and H $_2$ emission that have been observed from the remnant. A high density shell can be produced if the slow wind has passed through a termination shock induced by the pressure in the surrounding medium (§ 2.4). In this picture, the shell is elongated in the SW–NE direction, giving the apparent barrel shape of the strong X-ray and radio emission. The elongation to the SW, ahead of the shock wave, may show up as H $_2$ emission in this direction (Oliva et al. 1990). The radiative shock waves appear where the forward shock wave encounters the dense parts of the shell; Meaburn & Allan (1986) have noted that the velocities of the shocked region suggest interaction with dense condensations.

The X-ray emission is produced in somewhat lower density parts of the shell. The X-ray emission is strongest at the outer parts of the remnant and the temperature is relatively low. This

is expected for supernova interaction with a shell and is also observed in SN 1987A (McCray 2003).

An unusual aspect of RCW 103 is the H_2 emission from the vicinity of a young remnant. Although the emission has been interpreted as interaction with a molecular cloud (Oliva et al. 1990; Rho et al. 2001), there is no evidence that the remnant is embedded in a molecular cloud, and we suggest a circumstellar wind interpretation here. The presence of the H_2 would rule out the possibility that the progenitor of the supernova was a normal red supergiant, because of the energetic emission expected at the time of shock breakout. An alternative is a highly extended RSG, or one with a dense wind that can sustain a radiation dominated shock wave. An intriguing possibility is that the shock breakout radiation played a role in exciting the H_2 emission, which cannot be explained by the excitation from the current radiation field (Rho et al. 2001).

The presence of the extended dense wind in this picture places RCW 103 in the SN IIL/b category.

6.3. Puppis A

Puppis A has a remarkable morphology, with extended interstellar interaction, fast O-rich knots, and a central compact X-ray source. For a distance of 2 kpc, the full remnant diameter is 32 pc; the age derived from the motion of O-rich knots, assumed to be freely expanding, is 3700 yr (Winkler et al. 1988); the velocity range of the O-rich knots is $1500 - 3000 \text{ km s}^{-1}$.

An important clue to the supernova type comes from the fact that there is some H in the O-rich knot, even though the mass ratio of O/H is ~ 30 (Winkler & Kirshner 1985). The presence of a small amount of H at a velocity of $1500 - 3000 \text{ km s}^{-1}$ suggests a SN II in which the progenitor has undergone considerable mass loss, i.e. a SN IIL/b. The presence of some slow filaments with a N overabundance (Dopita, Mathewson, & Ford 1977) is consistent with material from the RSG wind of the progenitor. The fact that this gas has been shocked and cooled requires that it be gas that had passed through the termination shock of the RSG, or made up of clumps in the RSG wind. The RSG wind gas is expected to extend out to $\lesssim 7 \text{ pc}$ from the site of the supernova and it is a prediction of the present model that slow N-rich material should be present only in the central part of the remnant. The large diameter of Puppis A, 32 pc, implies that the outer interaction is with the interstellar medium. Blair et al. (1995) have analyzed emission from a shocked cloud on the eastern side of the remnant; the abundances are deduced to be close to solar. It is possible that N-rich ejecta filaments are also present and can range more widely in the remnant than the RSG wind gas. Winkler et al. (1989) found a N-rich filament with a velocity close to $1,000 \text{ km s}^{-1}$ in the central part of the remnant.

6.4. Kes 73

The young remnant Kes 73 is notable for containing an AXP (anomalous X-ray pulsar) with a period of 12 s (Vasisht & Gotthelf 1997), which is interpreted as a highly magnetized neutron star with $B \sim 10^{15}$ G. Sanbonmatsu & Helfand (1994) estimate a distance to the remnant between 6 and 7.5 kpc from HI absorption. The remnant radius of $4.7d_7$ pc and swept up mass of $\sim 8.8d_7^3 M_\odot$ (Gotthelf & Vasisht 1997) are consistent with a SN IIL/b running into the RSG wind lost from the progenitor star. The swept up mass is larger than would be expected for a SN 1987A-like remnant, although this possibility cannot be entirely ruled out. The models of § 4 suggest an age of 800 – 2000 yr.

6.5. 1E 0102.2–7219 in the SMC

The remnant E0102 (1E 0102.2–7219) is in the SMC (Small Magellanic Cloud) at an estimated distance of 59 kpc. No central compact object or related nebula have been identified and Gaetz et al. (2000) set an upper limit of $L_x < 9 \times 10^{33}$ erg s⁻¹ on the X-ray luminosity of a central PWN. Using the empirical relation between L_x and \dot{E} of Seward & Wang (1988), we have $\dot{E} \lesssim 2 \times 10^{36}$ erg s⁻¹. This is less than the spindown powers of pulsars in other young remnants (Table 1) and may indicate that the compact object is of the “quiet” variety, although a weak PWN remains a possibility.

The X-ray image of E0102 shows a bright ring of emission surrounded by a plateau with an outer edge (Gaetz et al. 2000). The ring can be identified with the reverse shock wave and the outer edge with the forward shock; detailed spectroscopic studies of the ring emission confirm that it is likely to be a reverse shock (Flanagan et al. 2004). The angular diameter of the forward shock is $44''$, corresponding to a radius of 6.3 pc at the distance of the SMC. The X-ray emission is at the inner boundary for a shell of optical emission which surrounds the remnant. This can be best seen in the *HST* image of Blair et al. (2000), which shows that the diameter of the emission is $\sim 60''$, or $R = 8.6$ pc. The ring of X-ray emission can be interpreted in terms of emission from pure heavy elements (Flanagan et al. 2004) and the remnant shows optical fast knots of O and Ne, but no H (Blair et al. 2000).

As in the case of Cas A, the evidence is strong that E0102 is interacting with the dense free wind from the progenitor star and is the result of a SN IIL/b. The forward shock wave is at 1.6 times the reverse shock, yet the outer emission does not show the strong limb brightening that would be expected if the shock were interacting with a constant density medium. The presence of heavy element-rich gas at the reverse shock is consistent with strong mass loss before the supernova. The outer ionized region can be attributed to wind material that was photoionized by the burst of radiation emitted at the time of shock breakout from a RSG progenitor. The observation of the He II line in the spectrum (Tuohy & Dopita 1983) is indicative of the hard photoionizing spectrum that is expected from shock breakout. The fact that the ionized wind extends out to a radius of 8.6 pc suggests that the surrounding pressure is relatively low (see eq. [11]), as might occur in the

SMC.

From proper motions at X-ray wavelengths, Hughes, Rakowski, & Decourchelle (2000) estimated a free expansion age of 1E0102 of 1000 yr. From the velocities of optical filaments, Eriksen et al. (2001) estimated an age of 2100 yr. In view of the relatively low velocities observed at both optical and X-ray (Flanagan et al. 2004) wavelengths, we prefer the large age. The low velocities also suggest that much of the supernova energy has been thermalized and it is approaching the blast wave phase. The comparison of the radius of 1E0102 with interaction models (Fig. 3) shows that the remnant is close to expectations.

Table 4 summarizes the properties of the remnants discussed in this section. They have all been identified with SN IIL/b, which can be attributed to the fact that these objects have the strongest interaction with the surrounding medium and are thus the brightest and best studied.

7. SUMMARY AND CONCLUSIONS

One aim of this paper is to relate the variety of young core collapse supernova remnants to the various kinds of supernovae. Four categories of supernovae have been identified, primarily based on the progenitor mass loss properties. The Type IIP progenitors are stars with mass $\sim 10 - 25 M_{\odot}$ that explode with most of their H envelope present. The mass loss that occurs during the RSG (red supergiant) phase remains close to the progenitor star; beyond it is a wind bubble created by the fast wind from the main sequence phase. During the supernova explosion, the core material is decelerated by the envelope, and H-rich material is mixed back to a velocity of a few 100 km s^{-1} or less.

The Type IIL/b events have had extensive mass loss from the H envelope, so that the envelope is unable to fully decelerate the core material during the explosion. The mass loss from the progenitor can extend out $5 - 7 \text{ pc}$ from the progenitor. Observations of a number of these supernovae has shown an overabundance of N, at least near the star, so this can be taken as an indication of RSG wind material. In these supernovae, material moving at several 1000 km s^{-1} has little or no H present. Radiation from the time of shock breakout may be able to completely ionize the surrounding circumstellar medium. The exact properties of breakout radiation depend on the initial photospheric radius of the supernova.

The next stage of mass loss is the development of a Wolf-Rayet star with a fast H-poor wind. The resulting supernova is of Type Ib/c. During the Wolf-Rayet phase, the fast wind is typically able to sweep up the RSG wind, which is left in clumps and at larger radii. Ionizing radiation is expected at the time of shock breakout, but it is not capable of fully ionizing the circumstellar material.

The final kind of supernova can be called SN 1987A-like. SN 1987A had a sufficiently massive H envelope to decelerate the core and to mix H down to $\lesssim 700 \text{ km s}^{-1}$, yet it exploded as a blue

supergiant, which led to an intermediate amount of ionizing radiation at the time of shock breakout. The circumstellar medium close to the star is complex, as can be seen in the current interaction in SN 1987A, but, on a timescale of 100’s of years, the interaction should be with the wind from the RSG phase. None of the young remnants show properties that point to a SN 1987A-like event. This is consistent with the fact that such events do not appear to contribute substantially to the extragalactic supernova rate, although they are of low luminosity. The relatively high metallicity of our Galaxy, compared to the Large Magellanic Cloud, could also be a factor.

Plausible supernova types for young remnants are given in Table 3. Two remnants, the Crab and 3C58, are identified with Type IIP. Both show slow moving H rich gas and appear to have low density surroundings. However, in neither case has the interaction with the surroundings been observed, which introduces some doubt into the identification. G292.0+1.8 and G11.2-0.3 show evidence for strong circumstellar interaction on a scale of 5–7 pc, which is the region expected to be occupied by the RSG wind in the case of a SN IIL/b. For G292.0+1.8, the lack of H in ejecta moving at $\sim 2000 \text{ km s}^{-1}$ is further evidence for this supernova identification.

The nebulae 0540–69, Kes 75, and MSH 15-52 are plausibly identified with Type Ib/c remnants. They all have expanded with an average velocity $\sim 10,000 \text{ km s}^{-1}$ to radii $> 10 \text{ pc}$, which is inconsistent with interaction with the dense wind expected around a Type IIL/b. In the cases of 0540–69 and MSH 15-52, there is evidence for N-rich clumps in the outer parts of the remnants which can be identified with RSG material that has been accelerated outward by interaction with the Wolf-Rayet progenitor wind. An expectation for this scenario is that the ejecta are lacking H, for which there is some evidence in the case of 0540–69.

Models for the PWNe are developed based on the assumption of interaction with normal supernova ejecta and the use of the minimum energy from synchrotron emission to set a constraint on the internal energy. Successful models for the observed nebulae have an internal energy which is within a factor of a few of the minimum energy. The models provide an estimate of age of the remnant. In the case of 3C58, the age is 3000 – 4000 yr, inconsistent with the identification of 3C58 as the remnant of SN 1181. The larger age is indicated by the internal energy in the PWN, the expansion of the PWN, and the mass of swept-up thermal gas, and is consistent with the relatively low expansion observed at optical and radio wavelengths. Models for the PWNe in MSH 15-52 and G11.2-0.3 are consistent with their identification the SN 185 and SN 386, respectively. The age of MSH 15-52 is better specified by the models than that of G11.2-0.3. In the case of G11.2-0.3, the external wind interaction is also consistent with the supernova identification.

The models allow estimates of the initial rotation periods of the pulsars, which are found to be in the range 10 – 100 ms (Table 3). The pulsars with current periods $> 100 \text{ ms}$ show evidence for substantial spindown in order to be consistent with the PWN properties. The initial periods show no strong trend with supernova type. Table 3 also shows that the magnetic fields of the pulsars are not related to the supernova type. The presence of pulsars in the remnants of the various supernova types and the similar properties of the central pulsars is an indication that the supernova types are

not a mass sequence, as would be expected in a single star origin for the supernovae. In a binary origin for a substantial fraction of Type IIL/b and Type Ib/c supernovae, they overlap with the masses of Type IIP events so that the core masses can be in a similar range.

The lack of a relation between pulsar properties and supernova type is also an indication that mass fallback is not an important process for the basic neutron star properties. The estimated initial rotation periods of the pulsars limits the amount of fallback that can occur at near the Keplerian velocity. However, even a minute amount of fallback is important for the composition of the neutron star atmosphere. A H rich atmosphere is commonly assumed for young neutron stars. In the Type IIL/b and Ib/c events, material falling on the neutron is likely to be lacking H.

A number of young remnants without normal pulsars as central objects appear to fall into the Type IIL/b category. However, the lack of Type IIP and Ib/c events may be simply due to the fact that these remnants have weak circumstellar interaction and are faint.

The PWNe discussed in the here have ages $\sim 10^3$ yr. The finding of PWNe in the light from supernovae with ages ~ 10 yr would directly solve the problem of identifying a PWN with a particular supernova type and would substantially extend the known evolutionary sequence of PWNe. In this context, the recent discovery of compact, central radio emission in the Type IIn SN 1986J (Bietenholz, Bartel, & Rupen 2004) is of special interest. The source shows an inverted spectrum with a turnover near 20 GHz, as expected for free-free absorption by material in the surrounding supernova. The amount of absorption to a central PWN depends on the density structure of the supernova (§ 2.1), and also on the physical conditions in the gas. Sensitive observations of supernovae at late times provide the opportunity to study very young PWNe.

I am grateful to Richard Mellon for contributing to the thin shell models for pulsar wind nebulae. Support for this work was provided in part by NASA grant NAG5-13272 and NSF grant AST-0307366. I am also grateful for the stimulating atmosphere provided by the ISSI (International Space Science Institute, Bern) workshop on the “Physics of Supernova Remnants in the XMM-Newton, Chandra and INTEGRAL Era.”

Table 1. Properties of Pulsars and their Nebulae

PSR	Supernova Remnant	Distance (kpc)	\dot{E}/I_{45} (ergs s ⁻¹)	P (ms)	$P/2\dot{P}$ (yr)	R_{PWN} (pc)	R_{SNR} (pc)
B0531+21	Crab	2	4.7×10^{38}	33	1240	2	–
J0205+64	3C 58	3.2	2.7×10^{37}	66	5390	3.3	–
B0540–69	N158A	50	1.5×10^{38}	50	1660	0.9	9
J1846–03	Kes 75	19	8.3×10^{36}	325	723	1.4	9.7
B1509–58	MSH 15-52	5.2	1.8×10^{37}	150	1700	5.5	19
J1124–59	G292.0+1.8	6	1.2×10^{37}	135	2890	3.5	7
J1811–19	G11.2–0.3	5	6.4×10^{36}	65	24,000	0.9	3.3
J1930+19	G54.1+0.3	~ 5	1.2×10^{37}	137	2890	1.2	–
J1119–61	G292.2–0.5	~ 6	2.3×10^{36}	408	1606	–	11

Table 2. Minimum internal energies of pulsar wind nebulae

Supernova Remnant	p_1	p_2	ν_b (Hz)	$L_{\nu b}$ (ergs s ⁻¹ Hz ⁻¹)	E_{min} (ergs)	Reference
Crab	1.6	3.0	1×10^{13}	9.5×10^{23}	6×10^{48}	1
3C 58	1.2	3.0	5×10^{10}	3.0×10^{23}	1×10^{48}	2
0540–69	1.5	2.6	2×10^{13}	3.0×10^{22}	5×10^{47}	1
Kes 75	1.0	3.0	1×10^{13}	1.2×10^{23}	1×10^{48}	3
MSH 15-52	1.4	3.1	3×10^{13}	4.4×10^{21}	1.5×10^{48}	4
G292.0+1.8	1.1	2.8	3×10^{10}	2.0×10^{23}	1×10^{48}	5
G11.2–0.3	1.5	2.46	8×10^9	7.8×10^{21}	3×10^{46}	6
G54.1+0.3	1.26	2.8	5×10^{11}	6.7×10^{21}	8×10^{46}	7

References: (1) Manchester et al. 1993; (2) Green & Scheuer 1992; (3) Blanton & Helfand 1996; (4) Gaensler et al. 2002; (5) Gaensler & Wallace 2003; (6) Roberts et al. 2003; (7) Lu et al. 2002.

Table 3. Properties deduced from models

Supernova Remnant	Supernova Type	Age (year)	P_0 (ms)	B (10^{12} G)
Crab	IIP	950	20	4
3C 58	IIP	3500	40	4
0540–69	Ib/c	800	40	5
Kes 75	Ib/c	1000	30	48
MSH 15–52	Ib/c	1700	10	14
G292.0+1.8	IIL/b	3200	40	10
G11.2–0.3	IIL/b	1600	60	2
G54.1+0.3	IIP,Ib/c	1500	100	10
G292.2–0.5	IIP,Ib/c	1700	$\ll 200$	41

Table 4. Properties of remnants without normal pulsars

Supernova Remnant	Distance (kpc)	Supernova Type	Age (year)	Radius (pc)
Cas A	3.4	IIL/b	320	2.5
RCW 103	3.8	IIL/b	–	5.0
Puppis A	2	IIL/b	3700	16
Kes 73	7	IIL/b	–	4.7
1E 0102	59	IIL/b	1000–2100	6.3

REFERENCES

- Bandiera, R., Pacini, F., & Salvati, M. 1983, *A&A*, 126, 7
- Basko, M. 1994, *ApJ*, 425, 264
- Bietenholz, M. F., Bartel, N., & Rupen, M. P. 2004, *Science*, 304, 1947
- Bietenholz, M. F., Kassim, N. E., & Weiler, K. W. 2001, *ApJ*, 560, 772
- Blair, W. P., Raymond, J. C., Long, K. S., & Kriss, G. A. 1995, *ApJ*, 454, L35
- Blair, W. P. et al. 2000, *ApJ*, 537, 667
- Blanton, E. L., & Helfand, D. J. 1996, *ApJ*, 470, 961
- Blinnikov, S., Chugai, N., Lundqvist, P., Nadyozhin, D., Woosley, S., & Sorokina, E. 2003, in *From Twilight to Highlight: The Physics of Supernovae*, Eds. W. Hillebrandt & B. Leibundgut, (Berlin: Springer), 23
- Bocchino, F., Warwick, R. S., Marty, P., Lumb, D., Becker, W., & Pigot, C. 2001, *A&A*, 369, 1078
- Bucciantini, N., Blondin, J. M., Del Zanna, L., & Amato, E. 2003, *A&A*, 405, 617
- Camilo, F., et al. 2000, *ApJ*, 541, 367
- Camilo, F., Lorimer, D. R., Bhat, N. D. R., Gotthelf, E. V., Halpern, J. P., Wang, Q. D., Lu, F. J., & Mirabal, N. 2002a, *ApJ*, 574, L71
- Camilo, F., Manchester, R. N., Gaensler, B. M., Lorimer, D. R., & Sarkissian, J. 2002b, *ApJ*, 567, L71
- Cappellaro, E., Barbon, R., & Turatto, M. 2004, in *IAU Colloquium 192, Supernovae: 10 Years of SN 1993J*, eds. J.M. Marcaide & K.W. Weiler (Berlin: Springer), in press (astro-ph/0310859)
- Cappellaro, E., Turatto, M., Benetti, S., Tsvetkov, D. Y., Bartunov, O. S., & Makarova, I. N. 1993, *A&A*, 273, 383
- Cappellaro, E., Turatto, M., Tsvetkov, D. Y., Bartunov, O. S., Pollas, C., Evans, R., & Hamuy, M. 1997, *A&A*, 322, 431
- Chevalier, R. A. 1977, in *Supernovae*, ed. D. N. Schramm (Dordrecht: Reidel), 53
- Chevalier, R. A. 1982, *ApJ*, 259, 302
- Chevalier, R. A. 1989, *ApJ*, 346, 847
- Chevalier, R. A. 2003, in *From Twilight to Highlight: The Physics of Supernovae*, Eds. W. Hillebrandt & B. Leibundgut, (Berlin: Springer), 299

- Chevalier, R. A. 2004, *AdSpR*, 33, 456
- Chevalier, R. A. & Emmering, R. T. 1989, *ApJ*, 342, L75
- Chevalier, R. A., & Fransson, C. 1992, *ApJ*, 395, 540
- Chevalier, R. A., & Imamura, J. N. 1983, *ApJ*, 270, 554
- Chevalier, R. A., & Oishi, J. N. 2003, *ApJ*, 593, L23
- Clark, D. H., & Stephenson, F. R. 1977, *The Historical Supernovae* (New York: Pergamon)
- Colgate, S. A. 1971, *ApJ*, 163, 221
- Crawford, F., et al. 2001, *ApJ*, 554, 152
- Dopita, M. A., Mathewson, D. S., & Ford, V. L. 1977, *ApJ*, 214, 179
- Dopita, M. A. & Tuohy, I. R. 1984, *ApJ*, 282, 135
- Dwarkadas, V. 2001, *JKAS*, 34, 243
- Elmhamdi, A., et al. 2003, *MNRAS*, 338, 939
- Eriksen, K. A., Morse, J. A., Kirshner, R. P., & Winkler, P. F. 2001, in *Young Supernova Remnants*, ed. S. S. Holt & U. Hwang (Melville: AIP), 193
- Fesen, R. A., Kirshner, R. P., & Becker, R. H. 1988, in *Supernova Remnants and the Interstellar Medium*, ed. R. S. Roger, & T. L. Landecker (Cambridge: Cambridge University Press), 55
- Fesen, R. A., Shull, M. J., & Hurford, A. P. 1997, *AJ*, 113, 354
- Flanagan, K. A., Canizares, C. R., Dewey, D., Houck, J. C., Fredericks, A. C., Schattenburg, M. L., Markert, T. H., & Davis, D. S. 2004, *ApJ*, 605, 230
- Frail, D. A., & Moffett, D. A. 1993, *ApJ*, 408, 637
- Fransson, C., & Chevalier, R. A. 1989, *ApJ*, 343, 323
- Fransson, C., et al. 2004, *ApJ*, submitted
- Gaensler, B. M., & Wallace, B. J. 2003, *ApJ*, 594, 326
- Gaensler, B. M., Arons, J., Kaspi, V. M., Pivovarov, M. J., Kawai, N., & Tamura, K. 2002, *ApJ*, 569, 878
- Gaensler, B. M., Brazier, K. T. S., Manchester, R. N., Johnston, S., & Green, A. J. 1999, *MNRAS*, 305, 724

- Gaetz, T. J., Butt, Y. M., Edgar, R. J., Eriksen, K. A., Plucinsky, P. P., Schlegel, E. M., & Smith, R. K. 2000, *ApJ*, 534, L47
- Garcia-Segura, G., Langer, N., & Mac Low, M.-M. 1996, *A&A*, 316, 133
- Ghavamian, P., Hughes, J. P., & Williams, T. B. 2002, *BAAS*, 34, 1248
- Gonzalez, M., & Safi-Harb, S. 2003a, *ApJ*, 583, L91
- Gonzalez, M., & Safi-Harb, S. 2003b, *ApJ*, 591, L143
- Gotthelf, E. V., Petre, R., & Vasisht, G. 1999, *ApJ*, 514, L107
- Gotthelf, E. V., & Vasisht, G. 1997, *ApJ*, 486, L133
- Gotthelf, E. V., Vasisht, G., Boylan-Kolchin, M., & Torii, K. 2000, *ApJ*, 542, L37
- Green, D. A. 2004, A Catalogue of Galactic Supernova Remnants, Mullard Radio Astronomy Observatory, Cavendish Laboratory, Cambridge, UK (available at “<http://www.mrao.cam.ac.uk/surveys/snrs/>”)
- Green, D. A., & Scheuer, P. A. G. 1992, *MNRAS*, 258, 833
- Green, D. A., Gull, S. F., Tan, S. M., & Simon, A. J. B. 1988, *MNRAS*, 231, 735
- Hamuy, M. 2003, *ApJ*, 582, 905
- Heger, A., Fryer, C. L., Woosley, S. E., Langer, N., & Hartmann, D. H. 2003, *ApJ*, 591, 288
- Helfand, D. J., Collins, B. F., & Gotthelf, E. V. 2003, *ApJ*, 572, 783
- Herant, M., & Woosley, S. E. 1994, *ApJ*, 425, 814
- Houck, J. C., & Fransson, C. 1996, *ApJ*, 456, 811
- Hughes, J. P., Rakowski, C. E., & Decourchelle, A. 2000, *ApJ*, 543, L61
- Hughes, J. P., Slane, P. O., Park, S., Roming, P. W. A., & Burrows, D. N. 2003, *ApJ*, 591, L139
- Hughes, J. P., et al. 2001, *ApJ*, 559, L153
- Hwang, U., Petre, R., Holt, S. S., & Szymkowiak, A. E. 2001, *ApJ*, 560, 742
- Iwamoto, K., Nomoto, K., Hoflich, P., Yamaoka, H., Kumagai, S., & Shigeyama, T. 1994, *ApJ*, 437, L115
- Iwamoto, K., Young, T. R., Nakasato, N., Shigeyama, T., Nomoto, K., Hachisu, I., & Saio, H. 1997, *ApJ*, 477, 865
- Jun, J.-I. 1998, *ApJ*, 499, 282

- Kaspi, V. M., Manchester, R. N., Siegman, B., Johnston, S., & Lyne, A. G. 1994, *ApJ*, 422, L83
- Kennel, C. F., & Coroniti, F. V. 1984, *ApJ*, 283, 694
- Kifonidis, K., Plewa, T., Janka, H.-T., & Müller, E. 2003, *A&A*, 408, 621
- Kirshner, R. P., Morse, J. A., Winkler, P. F., & Blair, W. P. 1989, *ApJ*, 342, 260
- Klein, R. I., & Chevalier, R. A. 1978, *ApJ*, 223, L109
- Kozma, C., & Fransson, C. 1998, *ApJ*, 497, 431
- Lu, F. J., Wang, Q. D., Aschenbach, B., Durouchoux, P., & Song, L. M. 2002, *ApJ*, 568, L49
- Lundqvist, P., & Fransson, C. 1996, *ApJ*, 464, 924
- Lyne, A. G., Pritchard, R. S., Graham-Smith, F., & Camilo, F. 1996, *Nature*, 381, 497
- Lyne, A. G., Pritchard, R. S., & Smith, F. G. 1988, *MNRAS*, 233, 667
- Manchester, R. N., Staveley-Smith, L., & Kesteven, M. J. 1993, *ApJ*, 411, 756
- MacFadyen, A. I., Woosley, S. E., & Heger, A. 2001, *ApJ*, 550, 410
- Manchester, R. N., Staveley-Smith, L., & Kesteven, M. J. 1993, *ApJ*, 411, 756
- Mathewson, D. S., Dopita, M. A., Tuohy, I. R., & Ford, V. L. 1980, *ApJ*, 242, L73
- Matzner, C. D., & McKee, C. F. 1999, *ApJ*, 510, 379
- Maund, J. R., Smartt, S. J., Kudritzki, R. P., Podsiadlowski, P., & Gilmore, G. F. 2004, *Nature*, 427, 129
- McCray, R. 2003, in *LNP Vol. 598: Supernovae and Gamma-Ray Bursters*, ed. K.W. Weiler (Berlin: Springer), 219
- Meaburn, J., & Allan, P. M. 1986, *MNRAS*, 222, 593
- Murdin, P., & Clark, D. H. 1979, *MNRAS*, 189, 501
- Murray, S. S., Slane, P. O., Seward, F. D., Ransom, S. M., & Gaensler, B. M. 2002, *ApJ*, 568, 226
- Nomoto, K., Iwamoto, K., & Suzuki, T. 1995, *Phys. Rep.*, 256, 173
- Nomoto, K., et al. 2001, in *Supernovae and Gamma-Ray Bursts*, eds. M. Livio, N. Panagia, & K. Sahu (Cambridge: CUP), p. 144
- Nomoto, K., Sugimoto, D., Sparks, W. M., Fesen, R. A., Gull, T. R., & Miyaji, S. 1982, *Nature*, 299, 803

- Oliva, E., Moorwood, A. F. M., & Danziger, I. J. 1990, *A&A*, 240, 453
- Ostriker, J. P., & Gunn, J. E. 1971, *ApJ*, 164, L95
- Pacholczyk, A. G. 1970, *Radio Astrophysics* (San Francisco: Freeman)
- Park, S., et al. 2002, *ApJ*, 564, L39
- Pastorello, A. et al. 2004, *MNRAS*, 347, 74
- Pavlov, G. G., Zavlin, V. E., Aschenbach, B., Trümper, J., & Sanwal, D. 2000, *ApJ*, 531, L53
- Pooley, D. et al. 2002, *ApJ*, 572, 932
- Reed, J. E., Hester, J. J., Fabian, A. C., & Winkler, P. F. 1995, *ApJ*, 440, 706
- Rees, M. J., & Gunn, J. E. 1974, *MNRAS*, 167, 1
- Reynolds, S. P. 1985, *ApJ*, 291, 152
- Reynolds, S. P., & Chevalier, R. A. 1984, *ApJ*, 278, 630
- Reynoso, E. M., Green, A. J., Johnston, S., Goss, W. M., Dubner, G. M., & Giacani, E. B. 2004, *PASA*, 21, 82
- Rho, J., Reach, W. T., Koo, B.-C., & Cambresy, L. 2001, in *Young Supernova Remnants*, ed. S. S. Holt & U. Hwang (Melville: AIP), 197
- Roberts, M. S. E., Tam, C. R., Kaspi, V. M., Lyutikov, M., Vasisht, G., Pivovarov, M., Gotthelf, E. V., & Kawai, N. 2003, *ApJ*, 588, 992
- Ruiz, M. T. 1983, *AJ*, 88, 1210
- Sanbonmatsu, K. Y., & Helfand, D. J. 1992, *AJ*, 104, 2189
- Schaller, G., Schaerer, D., Meynet, G., & Maeder, A. 1992, *A&AS*, 96, 269
- Seward, F. D., Harnden, F. R., Jr., Murdin, R., & Clark, D. H. 1983, *ApJ*, 267, 698
- Seward, F. D., & Wang, Z.-R. 1988, *ApJ*, 332, 199
- Shigeyama, T. & Nomoto, K. 1990, *ApJ*, 360, 242
- Shigeyama, T., Iwamoto, K., Hachisu, I., Nomoto, K., & Saio, H. 1996, in *IAU Colloq. 145: Supernovae and Supernova Remnants*, eds. R. McCray & Z. Wang (Cambridge: CUP), 129
- Slane, P., Helfand, D. J., van der Swaluw, E., & Murray, S. S. 2004, *ApJ*, in press (astro-ph/0405380)
- Smartt, S. J., Maund, J. R., Gilmore, G. F., Tout, C. A., Kilkeny, D., & Benetti, S. 2003, *MNRAS*, 343, 735

- Stephenson, F. R., & Green, D. A. 2002, *Historical Supernovae and their Remnants* (Oxford Univ. Press: Oxford)
- Tam, C., & Roberts, M. S. E. 2003, *ApJ*, 598, L27
- Tam, C., Roberts, M. S. E., & Kaspi, V. M. 2002, *ApJ*, 572, 202
- Torii, K., Tsunemi, H., Dotani, T., & Mitsuda, K. 1997, *ApJ*, 489, L145
- Torii, K., et al. 1999, *ApJ*, 523, L69
- Tuohy, I. R., & Dopita, M. A. 1983, *ApJ*, 268, L11
- van der Swaluw, E., & Wu, Y. 2001, *ApJ*, 555, L49
- van der Swaluw, E., Achterberg, A., Gallant, Y. A., & Tóth, G. 2001, *A&A*, 380, 309
- Van Dyk, S. D., Garnavich, P. M., Filippenko, A. V., Höflich, P., Kirshner, R. P., Kurucz, R. L., & Challis, P. 2002, *PASP*, 114, 1322
- Van Dyk, S. D., Li, W., & Filippenko, A. V. 2003, *PASP*, 115, 1289
- Vasisht, G., & Gotthelf, E. V. 1997, *ApJ*, 486, L129
- Wellstein, S., & Langer, N. 1999, *A&A*, 350, 148
- Winkler, P. F., & Kirshner, R. P. 1985, *ApJ*, 299, 981
- Winkler, P. F., Kirshner, R. P., Hughes, J. P., & Heathcote, S. R. 1989, *Nature*, 337, 48
- Winkler, P. F., Tuttle, J. H., Kirshner, R. P., & Irwin, M. J. 1988, *IAU Colloq. 101: Supernova Remnants and the Interstellar Medium*, ed. R. S. Roger & T. L. Landecker (Cambridge: CUP), 65
- Woosley, S. E. 1988, *ApJ*, 330, 218
- Zhang, W., Marshall, F. E., Gotthelf, E. V., Middleditch, J., & Wang, Q. D. 2001, *ApJ*, 554, L177

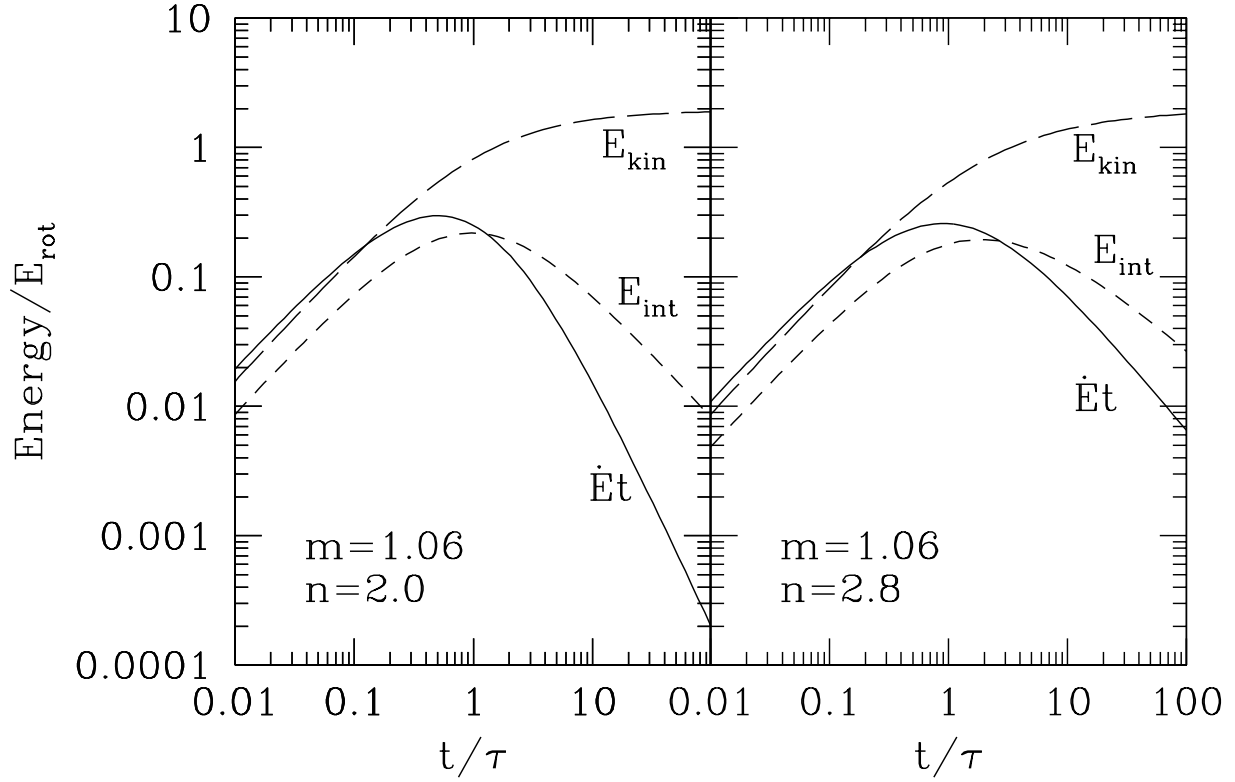


Fig. 1.— The evolution of pulsar nebula internal energy, E_{int} , kinetic energy of the swept-up shell, E_{kin} , and the current $\dot{E}t$ divided by the initial rotational energy, E_{rot} . The 2 models are characterized by the power law index of the supernova density profile, m , and the pulsar braking index, n . The reference time τ is the initial spindown time of the pulsar.

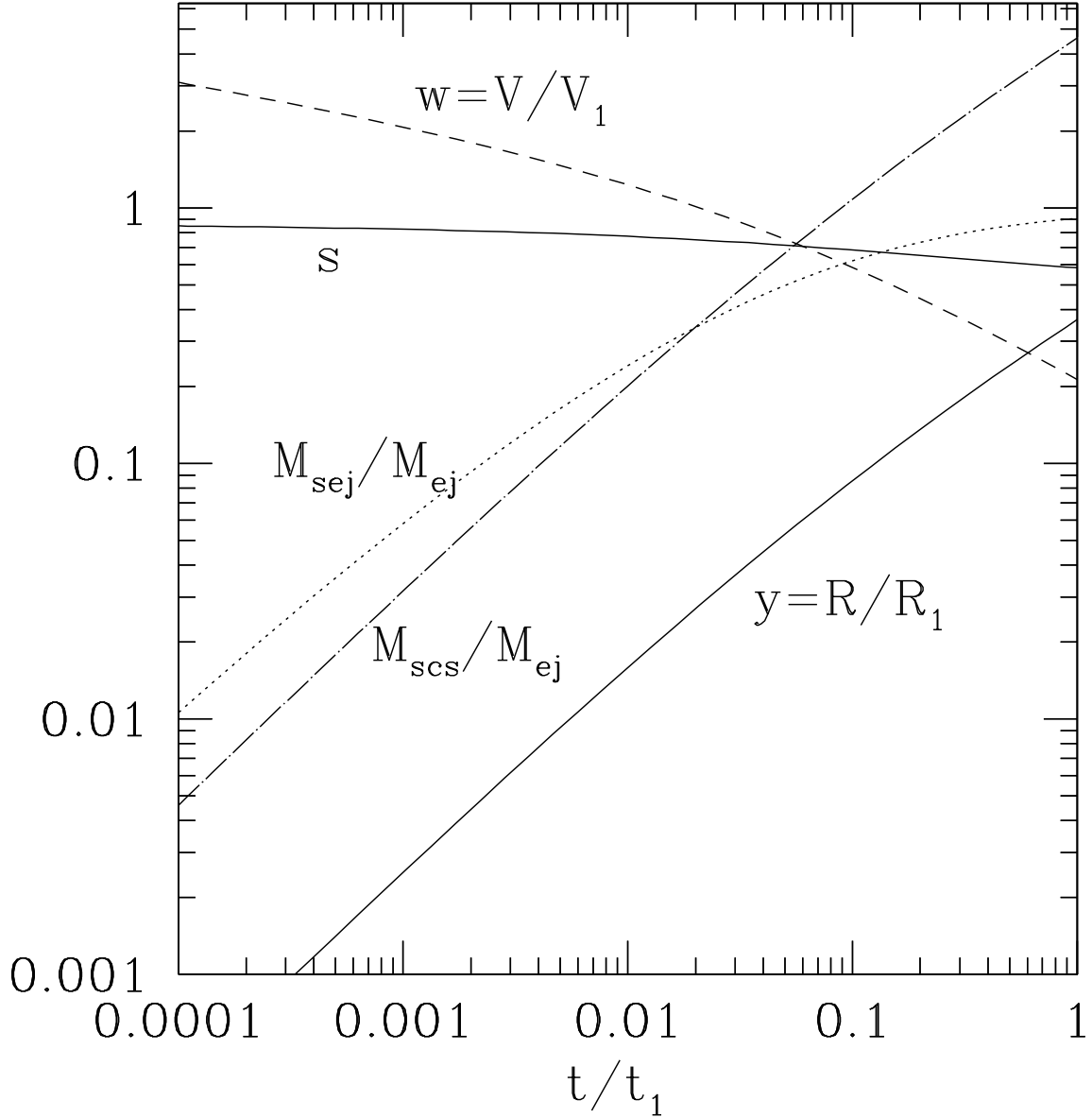


Fig. 2.— Results for the thin shell circumstellar interaction model described in § 4. The dimensionless variables y (radius) and w (velocity) are given as a function of time; s is the deceleration parameter for the shell. The swept up circumstellar mass, M_{scs} , and ejecta mass, M_{sej} , are given relative to the total ejecta mass, M_{ej} .

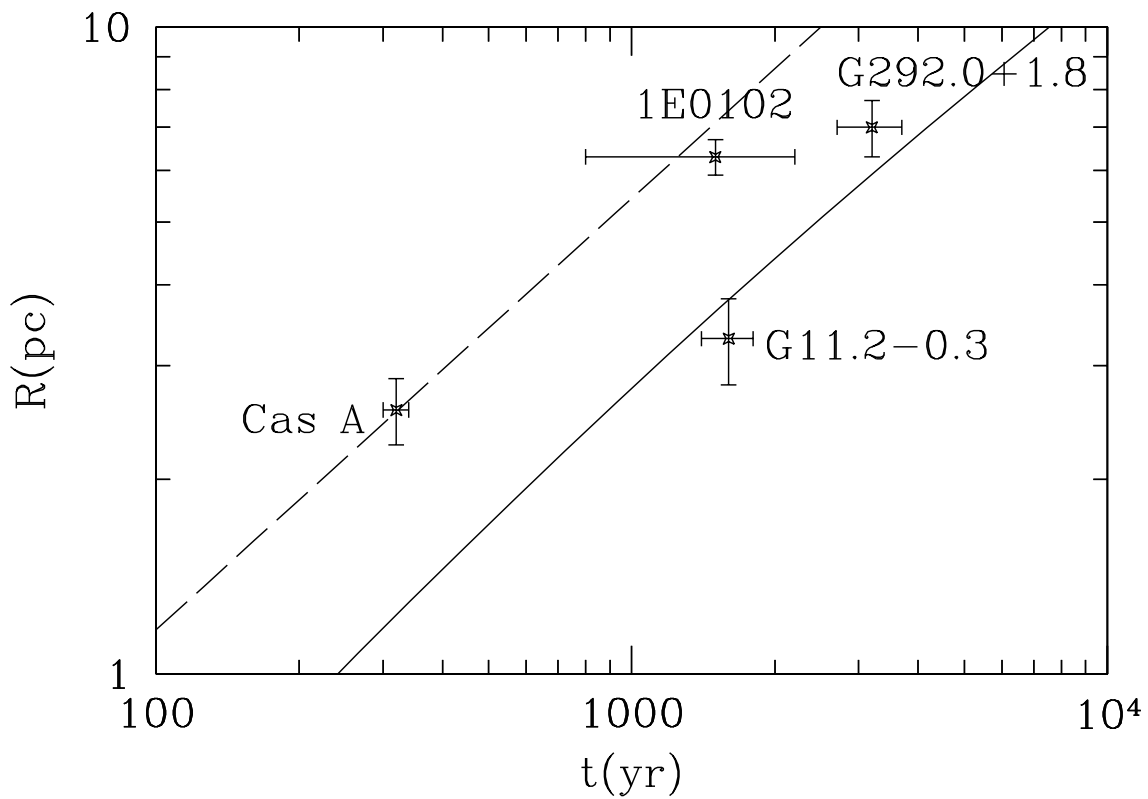


Fig. 3.— Models for thin shell expansion (solid line) and blast wave expansion (dashed line) in a circumstellar wind, using typical parameters (see § 4). The observational points are for young remnants that may be expanding in a wind.